NAVAL POSTGRADUATE SCHOOL
Monterey, California

Southern Hemisphere Application of the Systematic Approach to Tropical Cyclone Forecasting Part IV: Sources of Large Track Errors by Dynamical Models

by

Grahame Reader
Mark A. Boothe
Russell L. Elsberry
Lester E. Carr, III
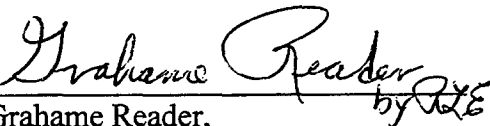
August 2000

20001204 062

Naval Postgraduate School
Monterey, California 93943

RADM David R. Ellison, USN   Richard Elster
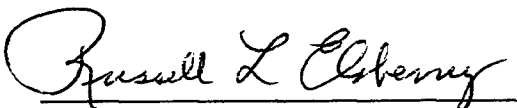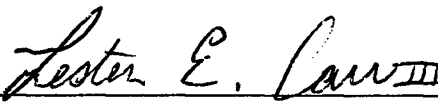Superintendent   Provost

This report was prepared by:
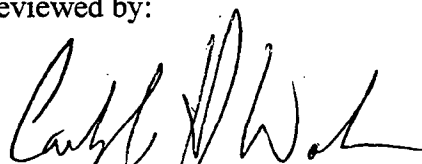
Grahame Reader,   Mark A. Boothe,
Bureau of Meteorology, Perth Australia   Meteorologist

Russell L. Elsberry   Lester E. Carr, III
Professor of Meteorology   Research Associate Professor of Meteorology

Reviewed by: Released by:

Carlyle H. Wash, Chairman   David W. Netzer
Department of Meteorology   Dean of Research

REPORT DOCUMENTATION PAGE

1. AGENCY USE ONLY (Leave blank)	2. REPORT DATE August 2000	3. REPORT TYPE AND DATES COVERED Interim 10/99 - 09/00

4. TITLE AND SUBTITLE
 Southern Hemisphere Application of the Systematic Approach to Tropical Cyclone Track Forecasting: Part IV. Sources of Large Track Errors by Dynamical Models
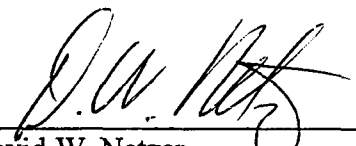
6. AUTHOR(S) Grahame Reader, Mark A. Boothe, Russell L. Elsberry, and Lester E. Carr, III

5. FUNDING

N0003900WRDF203

7. PERFORMING ORGANIZATION NAME(S) AND ADDRESS(ES)
 Naval Postgraduate School
 Department of Meteorology
 589 Dyer Rd., Room 254
 Monterey, CA 93943-5114

8. PERFORMING ORGANIZATION REPORT NUMBER

9. SPONSORING/MONITORING AGENCY NAME(S) AND ADDRESS(ES)
 SPAWARSYSCOM
 Code PMW 185
 San Diego, CA 92110-3127

10. SPONSORING/MONITORING AGENCY REPORT NUMBER

11. SUPPLEMENTARY NOTES
 The views expressed in this report are those of the authors and do not reflect the official policy or position of the Department of Defense.

12a. DISTRIBUTION/AVAILABILITY STATEMENT

 Approved for Public Release; Distribution Unlimited

12b. DISTRIBUTION CODE

13. ABSTRACT

Sources of 72-h track errors > 300 n mi by four dynamical model tropical cyclone predictions in the Southern Hemisphere during the 1997-98 and 1998-99 seasons are studied using conceptual models Carr and Elsberry have previously developed for the western North Pacific. Each of these conceptual models describes how the dynamical model incorrectly predicts a known physical cause of tropical cyclone motion. Midlatitude circulation-related error sources occur more frequently in the Southern Hemisphere, which is as expected since deeply penetrating midlatitude trough-ridge circulations have more of an effect on tropical cyclone motion. In addition to erroneous predictions of midlatitude cyclogenesis and anticyclogenesis, the dynamical models error in their response to midlatitude vertical wind shear and baroclinic cyclone interactions with the tropical cyclones. One frequently occurring tropical-related large track-error mechanism is Excessive-Direct Cyclone Interaction, which occurs for similar reasons in the Southern Hemisphere as in the western North Pacific study of Carr and Elsberry. Although this is a retrospective study of known large track errors, the ultimate goal is to help the forecaster detect likely erroneous tracks in real-time.

14. SUBJECT TERMS
 Topical cyclone track forecasting; Tropical cyclone motion; Dynamical tropical cyclone track errors.

15. NUMBER OF PAGES
 51

16. PRICE CODE

17. SECURITY CLASSIFICATION OF REPORT UNCLASSIFIED	18. SECURITY CLASSIFICATION OF THIS PAGE UNCLASSIFIED	19. SECURITY CLASSIFICATION OF ABSTRACT UNCLASSIFIED	20. LIMITATION OF ABSTRACT

ACKNOWLEDGMENTS

TABLE OF CONTENTS

LIST OF TABLES

LIST OF FIGURES

1. Introduction

a. Background

The long-range objective of the Systematic Approach to Tropical Cyclone (TC) Track Forecasting (hereafter the Systematic Approach) project of Carr and Elsberry (1994) has been to bring about significant quantitative and qualitative improvements in official TC track forecasts. Desired quantitative improvements include: lower average forecast track errors (FTE), official FTEs that are consistently better than the FTEs of the objective track forecast guidance available to the forecaster, and a reduction in the number of track forecasts that have very large FTEs (commonly referred to as "busts"). In addition, the meteorological reasoning of the forecaster is a highly important, albeit qualitative, component of the official track forecast. The Systematic Approach is designed to help the TC forecaster develop a meteorological basis for the official track forecast that reflects dynamically-sound, state-of-the-science understanding of TC motion and track prediction.

When the Systematic Approach was developed, the TC forecasters relied primarily on statistical and empirical guidance (Elsberry 1995). Although dynamical model guidance such as the Navy Operational Global Atmospheric Prediction System (NOGAPS) was available, nearly all of the models had systematic errors, e.g., a marked poleward bias for low-latitude TCs moving westward. In the original Systematic Approach concept, the plan had been to apply statistical adjustments to correct for systematic track errors in the dynamical model guidance for different synoptic patterns. A reduction in the systematic errors of the dynamical models used by the forecaster at that time would presumably have led to a reduction in the annual average track errors.

A major gain in the accuracy of the dynamical TC track forecast guidance for the forecaster has been achieved since 1994. First, the Geophysical Fluid Dynamics Laboratory (GFDL) model was demonstrated to provide superior guidance over the other statistical and empirical techniques (Kurihara *et al.* 1995). This regional model was subsequently modified to use the initial conditions and lateral boundary conditions from the NOGAPS model for provision of track forecast guidance in the western North Pacific and later in the Southern Hemisphere, and is referred to here as the GFDN model. Both the NOGAPS and the United Kingdom Meteorological Office (UKMO) global models were significantly improved in October 1994 by the introduction of improved TC synthetic observations (Goerss and Jeffries 1994; Heming *et al.* 1995). While TC track forecasts by the European Centre for Medium-range Weather Forecasts (ECMWF) are not directly available for operational use, rough estimates of the positions can be subjectively interpolated from the transmitted fields (For this research, the ECMWF provided high-resolution fields and Dr. Mike Fiorino provided objectively determined positions). Thus, two global (NOGAPS and UKMO) and one regional (GFDN) model tracks and fields are available for Southern Hemisphere TCs at the synoptic (0000 and 1200 UTC) and off-synoptic (0600 and 1800 UTC) times, respectively. The ECMWF model is integrated only once per day beginning at 0000 UTC. One special characteristic of the ECMWF model is that no synthetic observations are added to represent the TC structure or position.

1

One recent improvement in the dynamical model guidance has been the reduction in the systematic errors. J. Heming (UKMO, private conversation 2000) has shown that the annual average cross-track and along-track errors for all TC forecasts made by the UKMO model in the Northern and Southern Hemispheres have been reduced to near zero. Although Elsberry *et al.* (1999) have shown it is possible to apply a statistical adjustment to improve the NOGAPS tracks at 12 h through 36 h, no statistically significant improvement was achieved beyond 36 h. With the reduction in systematic errors, old rules about the performance of the models as a function of initial latitude or track orientation are not as valid. As this research has found (see examples in Elsberry and Carr 2000, Carr and Elsberry 2000 a, b), the same dynamical model that was good in one case (e.g., recurvature) can be the worst in another essentially identical case. Thus, the original Systematic Approach concept of applying statistical adjustments to the dynamical model tracks needed to be changed.

Although the dynamical models typically have skill relative to a climatology and persistence forecast, the dynamical models occasionally have large errors. For example, the distribution of 72-h NOGAPS, GFDN, UKMO, and ECMWF track forecast errors during the 1997-98 and 1998-99 Southern Hemisphere seasons are shown in Fig. 1.1. Notice that all of these model error distributions are skewed toward the larger errors. The mean/maximum 72-h track errors for the NOGAPS, GFDN, UKMO, and ECMWF models are 275/897 n mi, 303/772 n mi, 248/843 n mi, and 249/645 n mi, respectively. Notice that these are not homogeneous samples (sample sizes are 257, 193, 257, and 152). As sub-samples of all available 72-h forecasts, those with errors exceeding 300 n mi (defined in this study to be "large") are 34%, 49%, 29%, and 27%, respectively.

The new Systematic Approach focus is the reduction in the number of official track forecasts with large errors. Although not numerous during most seasons, these forecast "busts" provide such poor guidance to the customer that confidence is degraded. If these large errors could be eliminated, the warnings would be more consistent in time. Then the areas warned would be reduced so that customers in adjacent areas would not unnecessarily make preparations, and those customers in the warned areas could more confidently make the appropriate preparations.

The new overview of the Systematic Approach is illustrated in Fig. 1.2. In Phase I, the assessment of the current synoptic situation is based on the analyses, the TC information, and all observations, and uses the Meteorological Knowledge base. Bannister *et al.* (1997, 1998) and Reader *et al.* (1999) developed this Southern Hemisphere knowledge base. In Phase II, the evaluation of the dynamical model track forecasts is done with the aid of the Model Traits knowledge base that is the focus of this report. Still to be developed is the knowledge base to be used in the Phase III formulation of the official track forecasts.

b.   *Motivation*

The basic motivation for this work is to help the forecaster detect when the dynamical guidance is likely to be highly erroneous, and thus should be rejected during preparation of the warning. Elsberry and Carr (2000) have examined the track forecast errors as a function of the
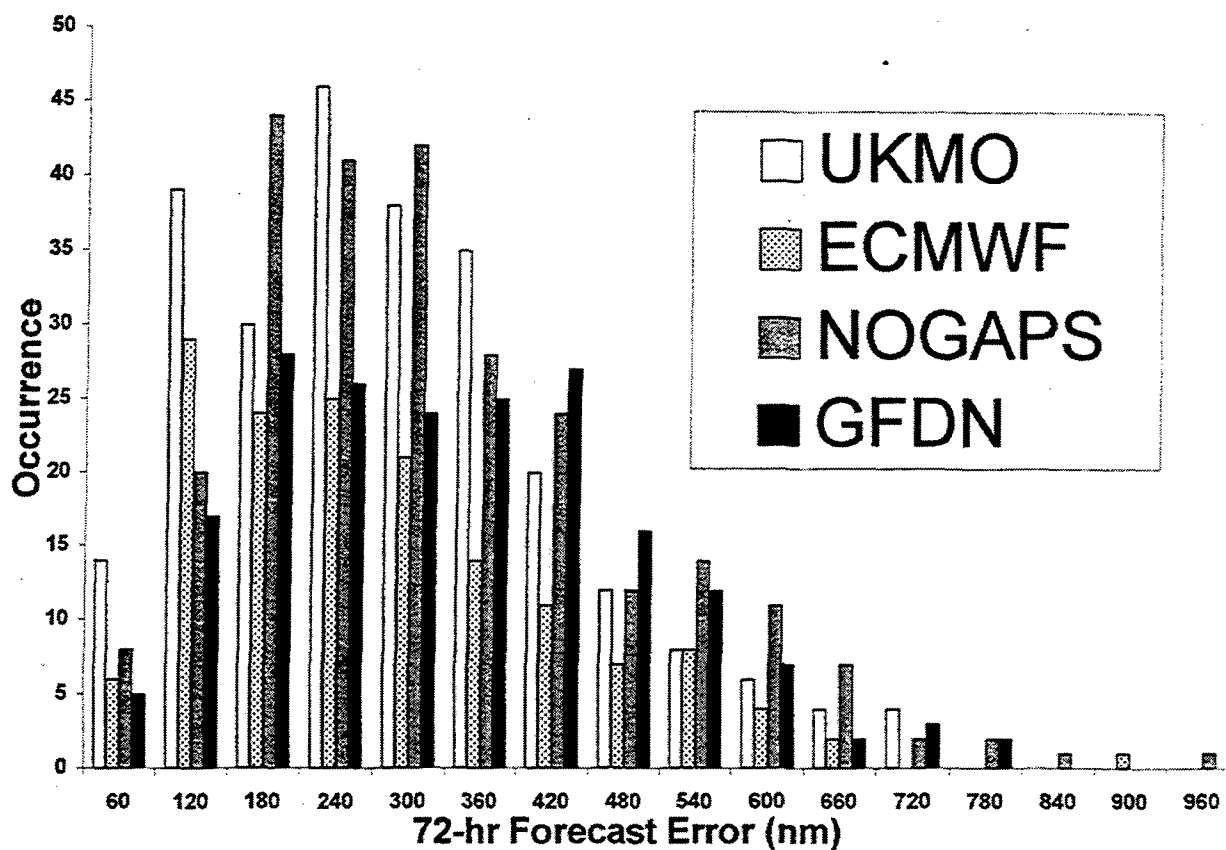
Fig. 1.1 Histograms of 72-h track errors for the NOGAPS, GFDN, UKMO, and ECMWF forecasts of Southern Hemisphere TCs during 1997-98 and 1998-99.

Systematic Approach
Conceptual Framework

PHASE	RESOURCES	TASKS	KNOWLEDGE BASES
I	Dynamical Model Analyses / TC Track / Observations and Imagery	Current Synoptic Situation Determination	TC Motion Meteorology / Imagery Interpretation
II	Dynamical Model Track and Field Forecasts / Objective Aid Track Forecasts	Dynamical Model Forecasts Evaluation	Dynamical Model Forecast Traits / Objective Aid Forecast Traits
III	Selected Dynamical Model Track and Field Forecasts / Objective Aid Track Forecasts	Official Forecast Track Formulation & Associated Prognostic Reasoning	Track Forecast Construction Rules / Confidence Estimation Techniques

Fig. 1.2 New overview of the Systematic Approach phases. The focus of this study is to develop a Dynamical Model Traits knowledge base for the Southern Hemisphere TCs.

4

spread (maximum distance to consensus centroid) among these five dynamical models. Their five-member consensus approach is an extension of the Goerss (2000) three-global model or two- regional model consensus technique at the synoptic and off-synoptic times, respectively. Goerss demonstrated that his consensus forecasts were either the best or the second-best guidance in about 70% of the forecasts. As might be expected based on experience with ensemble prediction systems, an average of five independent dynamical models with only small systematic errors provides an improvement over the three-member or two-member consensus. Although Elsberry and Carr (2000) documented that a small spread (< 300 n mi, or 555 km) among the five model tracks often implied a small consensus forecast error, in a sizeable fraction of the small spread cases the consensus error exceeded 300 n mi. Another important result was that a large spread among the five model tracks did not necessarily imply a large consensus track error, because the errors of two (or more) of the models may be compensating. Elsberry and Carr (2000) did demonstrate that a large spread implies that at least one of the dynamical models will have an error larger than that spread. They propose a *selective consensus* approach in which the model guidance suspected to have a 72-h error greater than 300 n mi is first eliminated prior to calculating the average of the remaining four model tracks. They demonstrate that simply omitting the worst of the five dynamical model tracks would indeed improve the selective consensus over the *non-selective consensus*.

c.   *Basis for this track error study.*

Carr and Elsberry (1999, 2000a, b) have established a procedure for searching for the large track error sources, and have developed seven error mechanism conceptual models that describe the evolution of the wind and/or sea-level pressure fields that accompany their sample of western North Pacific cases during 1997. Dunnavan *et al.* (2000) have extended the Carr and Elsberry study to include the 1998 season, and have also examined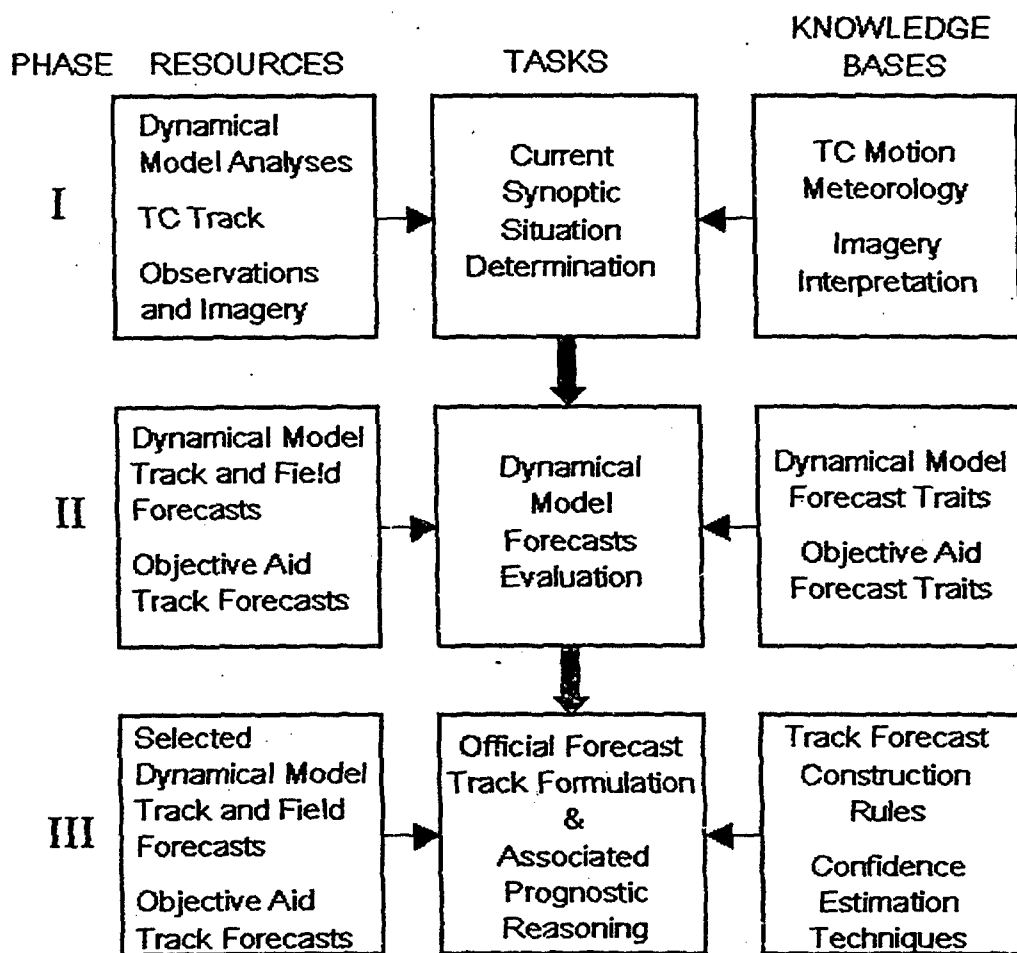 the UKMO and ECMWF model large track errors during the 1997 and 1998 seasons. Likewise, Brown *et al.* (2000) studied the large-track error sources for the NOGAPS, UKMO, and ECMWF models for Atlantic TCs during 1997-1998. The important conclusion from these two follow-on studies is that the same seven error mechanism conceptual models of the original Carr and Elsberry study accounted for the frequently occurring errors in other years, in another TC basin, and for two other models. Although this conclusion was not obvious, a possible explanation is that the basic physics of TC motion are the same, and if the models improperly handled those physics in the western North Pacific, the potential for the same error mechanisms exists in other basins. This is the basis for the present study of the large track error sources for Southern Hemisphere TCs.

The second important conclusion from the Carr and Elsberry (1999, 2000a, b) study is that the large track errors that predominantly occur in the tropical regions or may be related to midlatitude circulations could be attributed to the dynamical model improperly predicting one of the physical mechanisms known to cause TC motion. For example, Excessive Direct Cyclone Interaction (E-DCI) between a TC and an adjacent cyclone occurred during 1997 for 39 NOGAPS forecasts and for 31 GFDN forecasts for which the track errors exceeded 300 n mi. However, track-altering DCI actually occurred only two times during 1997 for these western North Pacific TCs, so that the forecaster can be rather confident that a DCI predicted by the NOGAPS or GFDN models will likely be erroneous.

A dynamical Model Traits knowledge base for the Systematic Approach has been developed as a result of a systematic evaluation by Carr and Elsberry (1999, 2000a, b) of the NOGAPS and GFDN TC track forecasts for the western North Pacific during 1997. They organize results in a preliminary Model Traits knowledge base, the first level of which is reproduced in Table 1.1. This level identifies the error mechanisms that frequently degrade NOGAPS and/or GFDN track forecasts. Each of these error mechanisms is described by a conceptual model in Carr and Elsberry (2000 a, b) because they frequently occur to an Excessive or Insufficient degree in the NOGAPS and/or GFDN forecasts.

An admitted shortcoming (vis-à-vis real-time forecasting) of the Carr and Elsberry (1999, 2000 a, b), Dunnavan et al. (2000), and Brown et al. (2000) studies is that it was known that a large (> 300 n mi) 72-h track error existed. Their objective was to search for the source of that error. A critical extension of this work was to demonstrate that such erroneous track error characteristics could be recognized, and associated error mechanism conceptual models could be applied, in a (simulated) real-time forecast scenario. As described by Carr et al. (2000), such a successful demonstration of the real-time detection of large track errors by dynamical models was accomplished for storms 19W through 30W in the western North Pacific during 1999. In the terminology introduced above, Carr et al. (2000) were able to form a selective consensus track after elimination of a likely erroneous model track(s) that had smaller errors than a non-selective consensus track of all the models. This demonstration is another important motivation for developing a corresponding set of error mechanism conceptual models for Southern Hemisphere TCs. This will lead to a real-time test as in Carr et al. (2000) during the 2000-2001 Southern Hemisphere season.

Table 1.1 Level 1 of the Model Traits knowledge base described by Carr and Elsberry (2000 a, b) indicating error mechanisms that frequently (F) degrade JTWC track forecast model guidance. The three letter abbreviations for the error mechanisms correspond to those in the western North Pacific Meteorological knowledge base (see Table 2.1) for acronyms. The prefixes stand for excessive (E) or insufficient (I) effects on the physical processes in the numerical forecast. In the rows for Beta and Advection Models (FBAM, MBAM, SBAM) and the CSUM, the designator F means frequently degraded when the NOGAPS forecast is degraded by the same error mechanism.

Model Name	Error	Mechanism	Frequency	Of	Occurrence		
	E-DCI	E-RMT	E-RTF	E-MCG	E-RVS	E-BCI	I-BCI
NOGAPS	F	F	F		F	F	F
GFDN	F			F		F	
BAMs	F	F	F			F	F
CSUM			F				

d.   Objective

The objective of this continuation of the Carr and Elsberry (1999, 2000 a, b) study is to search for the causes of large (> 300 n mi) 72-h track errors by the NOGAPS, GFDN, UKMO, and ECMWF models for Southern Hemisphere TCs during the 1997-98 and 1998-99 seasons. An attempt will be made to apply the same error mechanism conceptual models (except adapted for Southern Hemisphere flows and track direction anomalies) as in the Carr and Elsberry study. Case studies will be presented to serve as a guide for forecasters to use in detecting likely cases of large dynamical TC track errors.

2.   Methodology and overview

The approach has been to identify and analyze Southern Hemisphere causes during the 1997-98 and 1998-99 seasons with large (> 300 n mi) 72-h errors by the NOGAPS, GFDN, UKMO, and ECMWF models (Fig. 1.1). As emphasized by Carr and Elsberry (1999, 2000 a, b) the model analyses and forecast fields (not just the tracks) must be available to search for explanations of the large errors. The winds at 500 mb (to represent the deep tropospheric steering flow) and the sea-level pressures were the primary analyses and predictions used. When the TC intensity was only a tropical storm or tropical depression, the wind fields at 700 or 850 mb would be examined. If vertical wind shear effects were suspected, the 200-mb winds would be examined.

The Systematic Approach Meteorological knowledge base (see Appendix for definitions and Reader *et al.* 1999 for discussion) defines the synoptic pattern/region that describes the initial TC motion and includes any transitional mechanism that may be present. Thus, the first step in the search for the forecast error source was to review the initial synoptic classification and any transitional mechanism. If indeed such a synoptic pattern/region and a specific transition was occurring, an explanation for a large track error may be sought in an incorrect prediction of that environment, an improper transition, or an incorrect timing of that transition. As indicated in Table 1.1, all of the frequently occurring error mechanisms found by Carr and Elsberry (1999, 2000 a, b) in the western North Pacific were indeed either an excessive or insufficient prediction by the models of the transitional mechanisms.

A comparison of the large error sources for western North Pacific TCs (Dunnavan *et al.* 2000) and those in this Southern Hemisphere study is given in Table 2.1 to provide a context for the later discussion of individual error mechanisms. Whereas the prominent error mechanism in the western North Pacific is related to the Direct Cyclone Interaction (DCI), this mechanism is only the second-most frequent in the Southern Hemisphere. The less frequent occurrence of binary cyclones in the Southern Hemisphere, especially those close enough to be improperly predicted by the models, is consistent with this result. Just as in the North Pacific, none of the other six tropical region error mechanisms in Table 2.1 occurred with a frequency of at least 10%. Since none of these tropical region error mechanisms accounted for even 5% of the overall errors in the Southern Hemisphere, the frequencies in Table 2.1 may be somewhat changed when a larger sample of cases becomes available. As DCI is the only tropical region error mechanism that will be described in this report, the reader is referred to Carr and Elsberry (1999, 2000a) for further discussion of the other tropical region error mechanisms.

By far the dominant error source for this sample of Southern Hemisphere TC track forecasts arises from an incorrect prediction of the Midlatitude System Evolution (MSE). Bannister *et al.* (1997, 1998) and Reader *et al.* (1999) had emphasized the relatively more important effect in the Southern Hemisphere of vigorous, tilted troughs from the midlatitudes penetrating deep into the tropics such that the TC motion would be affected. Considering the sparcity of conventional observations over the South Hemisphere oceans, and the extent of these trough-ridge penetrations into the tropics, it is not surprising that the four prediction models in

this study may not handle well this physical mechanism for affecting TC motion. Two other important error mechanisms are also related to the midlatitude circulation, namely the Response to Vertical Wind Shear (RVS) with about 12% and Baroclinic Cyclone Interaction (BCI) with about 9% of all cases (Table 2.1). Consequently, about 66% of the large track errors could be attributed to midlatitude circulation influences, versus about 33% for primarily tropical errors.

Table 2.1 Overall comparison between large error (> 300 n mi) sources detected for four dynamical models in the western North Pacific during the 1997 and 1998 seasons versus in the Southern Hemisphere in this study during the 1997/1998 and 1998/1999 seasons. The asterisks indicate error sources that primarily occur while the TC is still in the tropics.

Error Source	North Pacific		Southern Hemisphere	
	Number	Percent	Number	Percent
Direct Cyclone Interaction*	70	35.3	49	20.3
Semi-direct Cyclone Interaction*	4	2.0	6	2.5
Indirect Cyclone Interaction*	4	2.0	5	2.1
Ridge Modification by a TC*	15	7.6	12	5.0
Reverse Trough Formation*	12	6.1	5	2.1
Equatorial Westerly Wind Burst*	0	0	1	0.4
Response to Vertical Wind Shear	14	7.1	28	11.6
Baroclinic Cyclone Interaction	33	16.7	22	9.2
Midlatitude System Evolution	28	14.1	108	44.8
Tropical Cyclone Size*	14	7.1	2	0.8
Not discernable	4	2.0	3	1.2
Total	**198**	**100.0**	**241**	**100.0**
Primarily tropical errors*	119	60.1	80	33.2
Midlatitude circulation influences	75	37.9	158	65.6
Not discernable	4	2.0	3	1.2

In only three of the 241 cases in this sample was the source of the large track error not discernable (Table 2.1). Thus, it was possible in all except about 1% of the cases to identify the sources of these Southern Hemisphere large track errors as one of the same error mechanisms that Carr and Elsberry (1999, 2000a, b) defined based on the western North Pacific sample. One case with a new error mechanism is related to the Equatorial Westerly wind Burst (EWB), which is a transitional mechanism that has so far only been identified in the Southern Hemisphere (Bannister et al. 1998).

A more detailed breakdown of the Southern Hemisphere large track error sources for the four models, whether the error was due to an excessive or an insufficient prediction of the transitional mechanism, and with a further subdivision of certain error mechanisms is given in Table 2.2. One important characteristic for the DCI mechanism is that it is about 15 times more likely to occur in an excessive mode as in an insufficient mode. Whereas excessive RVS is an exclusive mechanism of the three global models (NOGAPS, UKMO, and ECMWF), insufficient RVS is exclusive for the regional (GFDN) model. No preference for excessive versus insufficient exists for the BCI or the overall MSE error mechanisms. The breakdown of the

Table 2.2 Percentages of all poor forecasts as in Table 2.1, except relative to each of the four models subdivided as to whether the error mechanism is excessive (E) or insufficient (I), and with more breakdowns for certain error mechanisms.

CAUSES OF DEGRADED TRACK FORECASTS DURING 1997/8 & 1998/9		PERCENT OF 72-H TRACK FORECASTS - WITH ERROR>300 N MI									
Phenomenon Name		NOGAPS E	NOGAPS I	GFDN E	GFDN I	UKMO E	UKMO I	ECMWF E	ECMWF I	ALL MODELS E	ALL MODELS I
Direct Cyclone Interaction (DCI)	DCI	27.3%	3.9%	13.6%		17.7%		11.1%	3.7%	18.6%	1.2%
Semi Direct Cyclone Interaction (SCI)	SCI	1.3%	1.3%		1.2%	3.2%			3.7%	1.2%	1.2%
SCI on Western TC	SCIW	1.3%	1.3%							0.4%	0.8%
SCI on Eastern TC	SCIE					3.2%				0.8%	
SCI on Poleward TC	SCIP										
SCI on Equatorward TC	SCIQ				1.2%						0.4%
Indirect Cyclone Interaction (ICI)	ICI	1.3%			1.2%	3.2%	1.6%			1.2%	0.8%
ICI on Eastern TC	ICIE	1.3%					1.6%			0.4%	0.4%
ICI on Western TC	ICIW				1.2%	3.2%	1.2%			0.8%	0.4%
Ridge Modification by TC	RMT	3.9%		8.6%			3.2%			4.0%	0.8%
Reverse Trough Formation	RTF		1.3%	1.2%			3.2%		3.7%	0.4%	1.6%
Equatorial Westerly Wind Burst	EWB							3.7%		0.4%	
Response to Vertical wind Shear	RVS	18.2%			3.7%	12.9%		11.1%		10.1%	1.2%
Baroclinic Cyclone Interaction	BCI	3.9%	3.9%	2.5%		4.8%	11.3%	11.1%	3.7%	4.5%	4.5%
Midlatitude System Evolutions	MSE	9.1%	23.4%	38.3%	23.5%	17.7%	17.7%	29.6%	11.1%	23.1%	20.6%
Midlatitude CycloGenesis	MCG	5.2%	10.4%	25.9%	4.9%	4.8%	12.9%	18.5%	3.7%	13.4%	8.5%
Midlatitude CycloLysis	MCL		5.2%		7.4%						4.0%
Midlatitude AnticycloGenesis	MAG	3.9%	5.2%	11.1%	7.4%	12.9%	4.8%	11.1%	3.7%	9.3%	5.7%
Midlatitude AnticycloLysis	MAL		2.6%	1.2%	3.7%				3.7%	0.4%	2.4%
Tropical Cyclone Size	TCS							7.4%			0.8%
Not discernable							3.2%		3.7%		1.2%
Fields not available			1.3%		6.2%						2.4%

9

MSE mechanisms into Midlatitude CycloGenesis (MCG), CycloLysis (MCL), AnticycloGenesis (MAG), and AnticycloLysis (MAL) have tendencies toward excessive for the two genesis mechanisms (especially E-MCG in the GFDN model) and toward insufficient for the lysis mechanisms. Finally, notice that only the ECMWF model had an insufficient Tropical Cyclone Size (TCS), which is not surprising as that is the only model in which synthetic observations are not inserted to represent the TC structure and position.

Given this overview of the error mechanisms, several of the more important mechanisms will be discussed in subsequent chapters, starting with the midlatitude circulation error sources in Chapter 3. One tropical region error source will be described in Chapter 4.

3. Midlatitude circulation error sources

a. Description of Midlatitude System Evolution conceptual model

The fundamental idea of Midlatitude System Evolutions (MSE) is one of changes to the TC steering flow due to development, dissipation, and/or movement of midlatitude circulations (cyclones, troughs, or ridges) that occur essentially *independent of the TC*. This distinction will be more evident when the Baroclinic Cyclone Interaction (BCI) error source is discussed in the next section. Whereas in the MSE physical mechanism the primary effect is an advection by a modified steering current, the TC structure involved in a BCI are significantly modified by a baroclinic interaction (also called extratropical transition) as well as a track modification.

Idealized conceptual models for the four basic kinds of MSE are illustrated in Fig. 3.1. When Midlatitude CycloGenesis (MCG) takes place, the TC labeled A in Fig. 3.1a that has been tracking essentially westward in the Standard/Tropical Easterlies (S/TE) pattern/region [see Appendix and Reader *et al*. 1999 for discussion] equatorward of the subtropical ridge (STR) axis may be turned onto a more poleward heading as the developing midlatitude trough or cyclone "breaks" the ridge and creates more poleward flow in the vicinity of the TC (Fig. 3.1b). That is, sufficient MCG may result in an environment structure transition from the S/TE to the Standard/Poleward Flow (S/PF) pattern/region. Similarly, a TC that is poleward of the STR axis (Fig. 3.1a; labeled B) and moving east-southeastward in the Midlatitude (M) pattern and MW region when MCG takes place may then undergo directional and/or speed changes as the developing trough/cyclone alters the direction and strength of the midlatitude flow in which the TC is embedded (Fig. 3.1b). If MCG changes only the translation speed of the TC, then it will remain in the M/PF pattern/region, or perhaps change to the M/Midlatitude Westerlies (M/MW) pattern/ region. However, a vigorous MCG may change the direction of environmental steering sufficiently that a region transition may occur within the M pattern (e.g., from the MW to the PF region as suggested in Fig. 3.1b). For simplicity of depiction, Midlatitude CycloLysis (MCL) is depicted in Fig. 3.1 as the reverse of MCG. If MCG (MCL) occurs to a greater or lesser extent in a numerical TC forecast model than in reality such that a significant track error results, the Excessive (E) or Insufficient (I) MCG (MCL) is considered to have occurred.

When Midlatitude AnticycloGenesis (MAG) takes place, a TC labeled C in Fig. 3.1c that has been tracking southwestward in the S/PF pattern/region northeast of a weakness in the STR may be turned westward (or even north of west) as the developing midlatitude ridge/anticyclone increases the strength of the STR poleward of TC C. If the STR builds sufficiently in association with MAG, then TC C will be subjected to predominantly easterly or even southeasterly steering (Fig. 3.1d), i.e., may have a change in environment structure from the S/PF to the S/TE or S/Equatorward Flow (EF) pattern/region (see Fig. A-1 in Appendix for definitions). When such a MAG event takes place, the TC labeled D in Fig. 3.1c that has been moving eastward and/or poleward in the midlatitude flow poleward of the STR axis may undergo directional and/or speed changes as the developing midlatitude ridge/anticyclone alters the direction and strength of the midlatitude flow in which the TC D is embedded. If MAG changes only the translation speed of the TC D, then it will remain in either a M/PF or M/MW pattern/region. If MAG changes the direction of environmental steering sufficiently, then a region transition can occur within the M pattern (e.g., from the MW to the EF region as suggested in Fig. 3.1d). For simplicity,

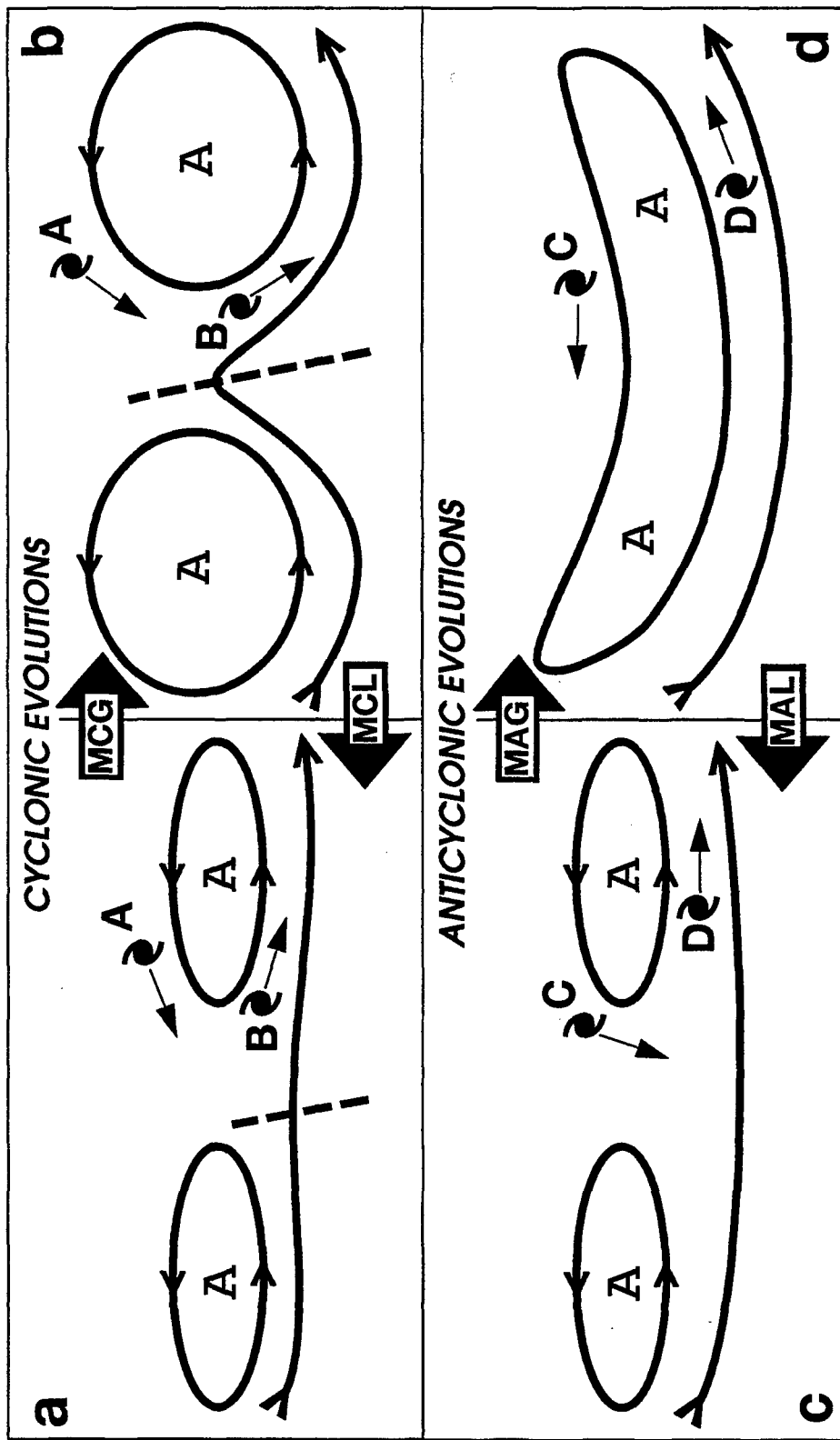11

Midlatitude System Evolutions (MSE)

Fig. 3.1. Schematics of the Midlatitude System Evolutions (MSE) that may lead to large TC track errors. The deepening of the midlatitude trough from panel a to panel b depicts Midlatitude CycloGenesis (MCG) and the reverse order (panel b to panel a) implies Midlatitude CycloLysis (MCL). Similarly, the midlatitude anticyclone change poleward of the TC from panel c to panel d depicts Midlatitude AntycyloGenesis (MAG) and the reverse order (panel d to panel c) implies Midlatitude AnticycloLysis (MAL).

12

Midlatitude AnticycloLysis (MAL) is simply treated as the reverse of MAG in Fig. 3.1. If MAG (MAL) occurs to a greater or lesser extent in a numerical TC forecast model than in reality such that a significant track error results, then *Excessive (E)* or *Insufficient (I)* MAG (MAL) is considered to have occurred.

In the schematics of Fig. 3.1, the midlatitude circulations are depicted as developing without moving. Actually, it may primarily be the approach or retreat of a non-developing midlatitude trough or ridge that causes a change in the steering flow and thus in the TC motion. Thus, either translation or development of midlatitude circulations will be considered as potential methods to affect the steering flow on the TC. It is also emphasized that a variety of TC track changes can occur depending on the location of the TC relative to the pertinent midlatitude circulations, and depending on changes in the amplitude and/or orientation of the midlatitude circulations. That is, the four MSE depictions in Fig. 3.1 should be considered as flexible templates that may have to be adjusted with respect to shape, location, and number of midlatitude circulations to explain particular TC tracks, or as it may be predicted by a dynamical model.

This MSE conceptual model in Fig. 3.1 is used for explaining differences between a model forecast and the movement of the TC, or between two dynamical model track forecasts, for situations in which TC interaction with its environment does not seem to be a determining factor in the motion. Note that when a MSE process alters the motion of a TC equatorward of the STR axis (e.g., TCs labeled A and C), it is by indirectly altering the structure of the STR in the vicinity of the TC. Even though the TC in this case is still in the tropics, the mechanism that is affecting the motion change is a midlatitude effect, and thus is not listed as a tropical effect in Tables 2.1 and 2.2.

b.   *Case study of Excessive Midlatitude Cyclogenesis (E-MCG)*

As indicated in Table 2.2, the GFDN model was most affected by E-MCG, and this excessive mode of MCG was about five times as likely as for the insufficient mode. The ECMWF model E-MCG errors are also five times as likely as I-MCG errors. Indeed, E-MCG is the most frequent error mechanism category for this small sample of ECMWF track errors. By contrast, the NOGAPS and UKMO models tend to have twice the number of I-MCG errors as E-MCG errors.

A case study for the GFDN track forecast of TC Thelma initiated at 1800 UTC 9 December 1998 is selected to illustrate some characteristic features in the 500-mb wind (Fig. 3.2) and sea-level pressure (Fig. 3.3) analyses and predictions. Thelma had started to turn to a more poleward track at the initial time, but on 12 December the storm had begun to move toward the southwest (Fig. 3.2a). Although the GFDL forecast path was excellent until the southwestward turn, the translation speed was excessive, and the 72-h position was well poleward of the verifying position.

At the time (1200 UTC 9 December) of the corresponding NOGAPS guidance (Fig. 3.2e), Thelma was a 130-kt TC just off the northwest Australian coast. The environmental flow features around Thelma are identical in the initial GFDN (Fig. 3.2I) and NOGAPS analyses,
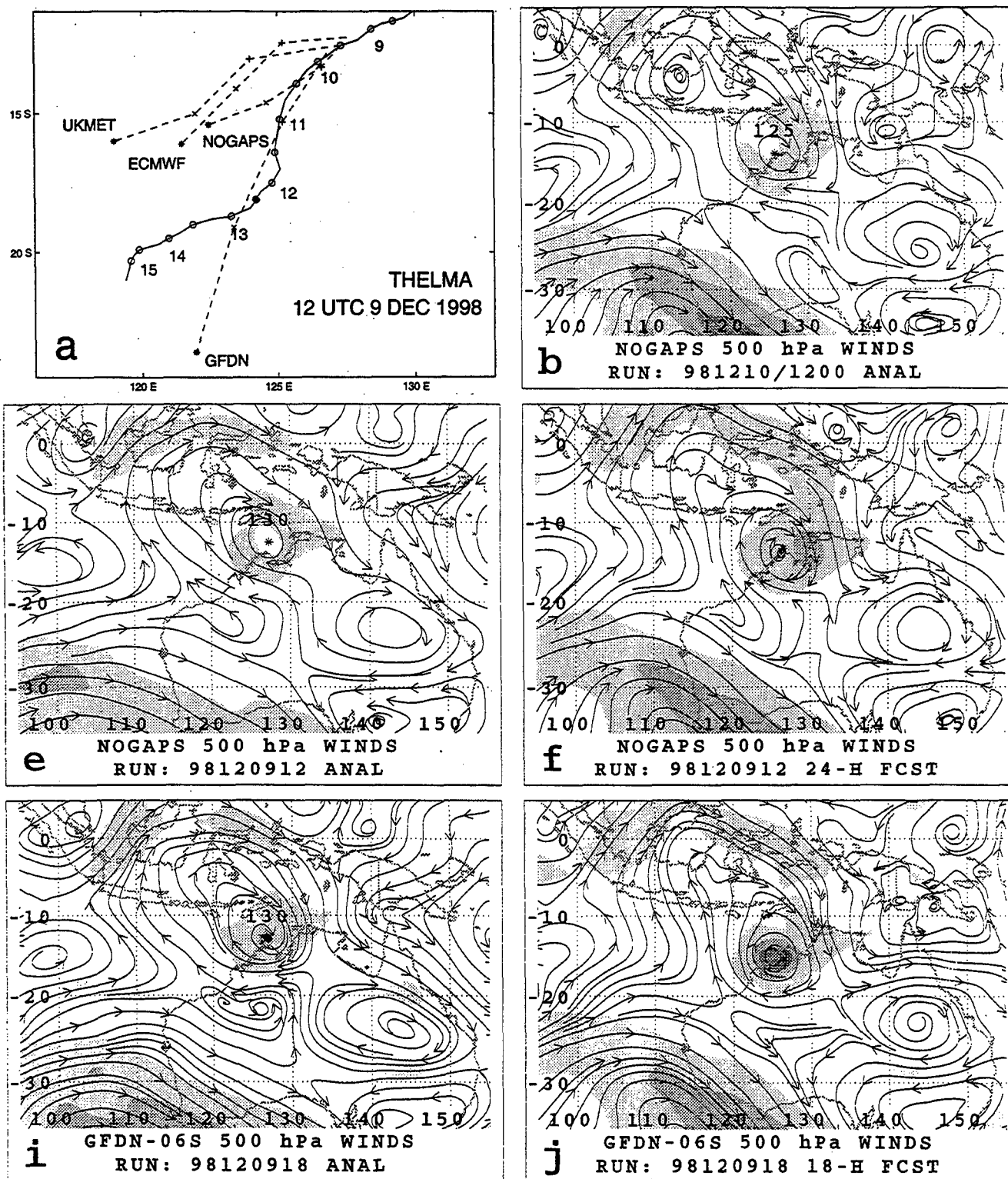
Fig. 3.2. (a) Track of TC Thelma (06) and forecast tracks by selected models (see insert), with the global models beginning at 1200 UTC 9 December 1998 and the regional models at 1800 UTC 9 December. The 24- (plus), 48- (cross), and 72-h (asterisk) positions are shown for the global models, and the 18-, 42-, and 66-h positions for the regional models. Panels (b)-(d) are the verifying NOGAPS 500-mb streamlines/isotachs, panels (e)-(h) are the 00-, 24-, 48-, and 72-h NOGAPS forecasts, and panels (i)-(l) are the 00-, 18-, 42-, and 66-h GFDN forecasts. Isotach shading starts at 20 kt and the increment is 10 kt. For the analyses, the asterisk is the JTWC position and an intensity is given only for the GFDN forecasts.
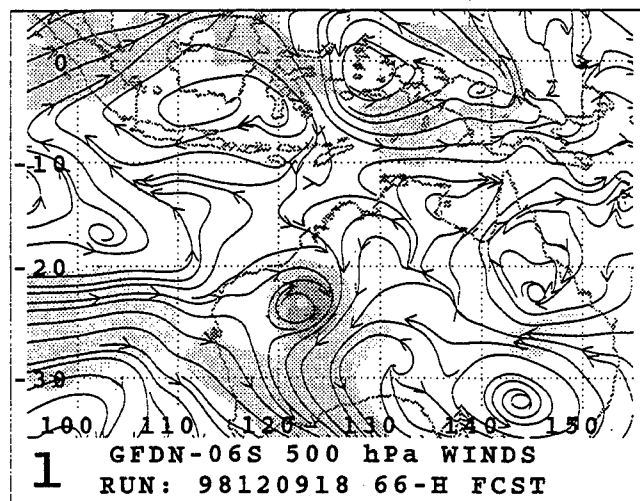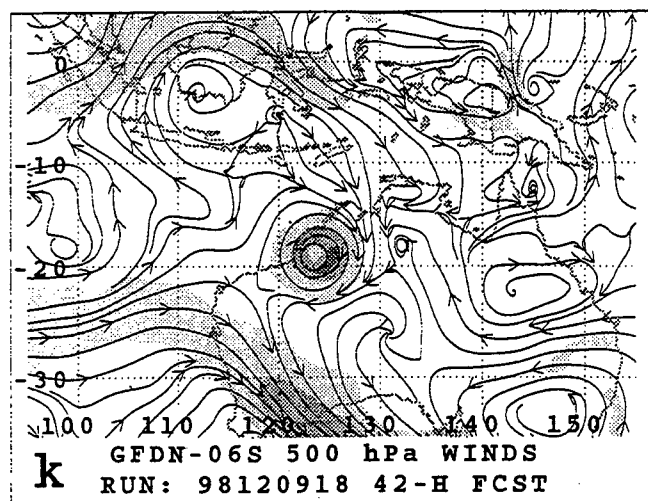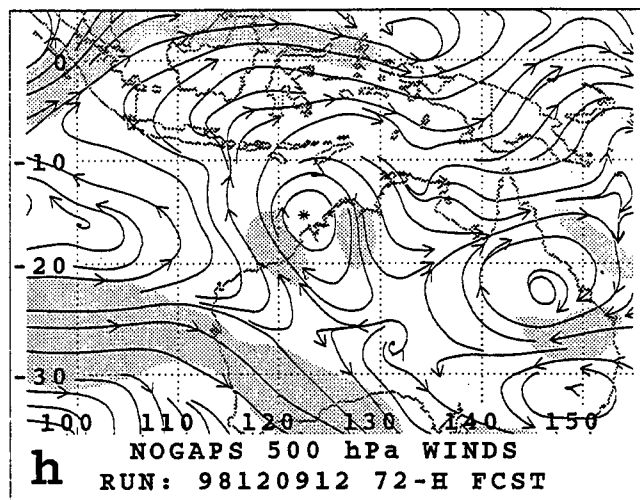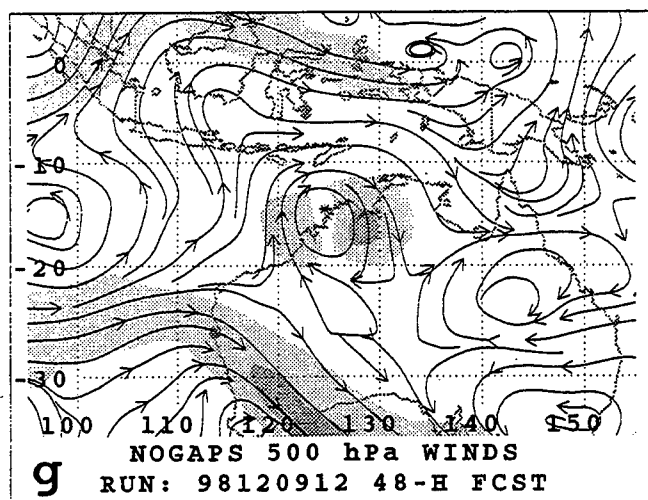
14
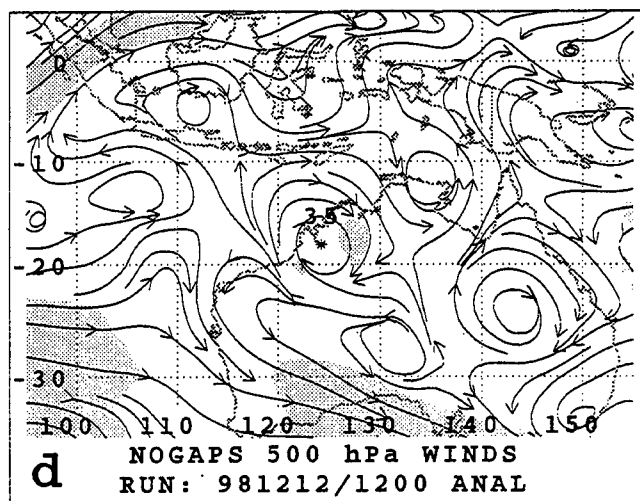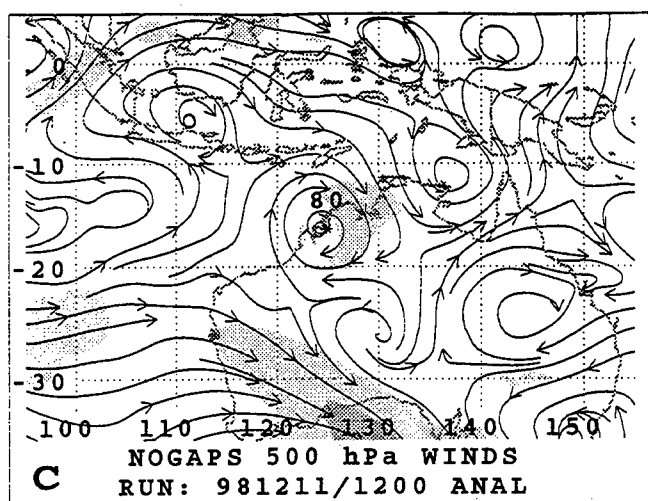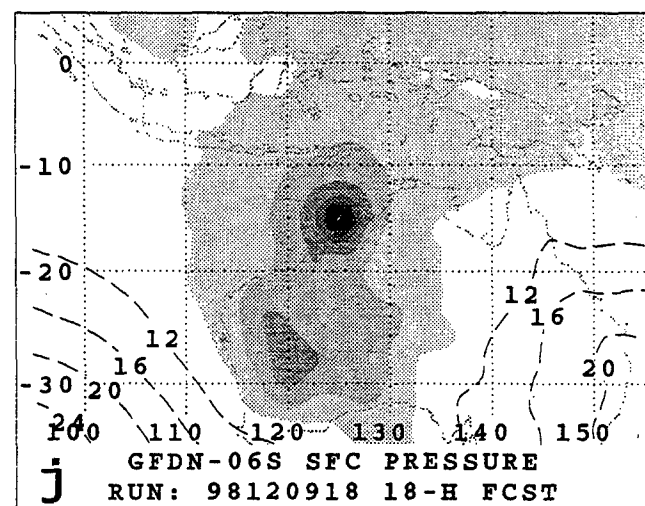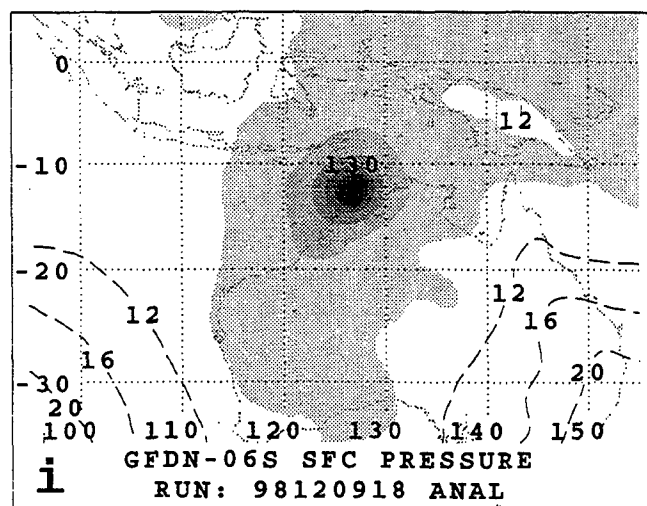
Fig. 3.2. (continued)

Fig. 3.3. As in Fig. 3.2, except for sea-level pressure (shading starts at 1008 mb and the increment is 4 mb).

NOGAPS SFC PRESSURE
RUN: 981211/1200 ANAL

NOGAPS SFC PRESSURE
RUN: 981212/1200 ANAL

NOGAPS SFC PRESSURE
RUN: 98120912 48-H FCST

NOGAPS SFC PRESSURE
RUN: 98120912 72-H FCST

GFDN-06S SFC PRESSURE
RUN: 98120918 42-H FCST

GFDN-06S SFC PRESSURE
RUN: 98120918 66-H FCST

Fig. 3.3. (continued)

17

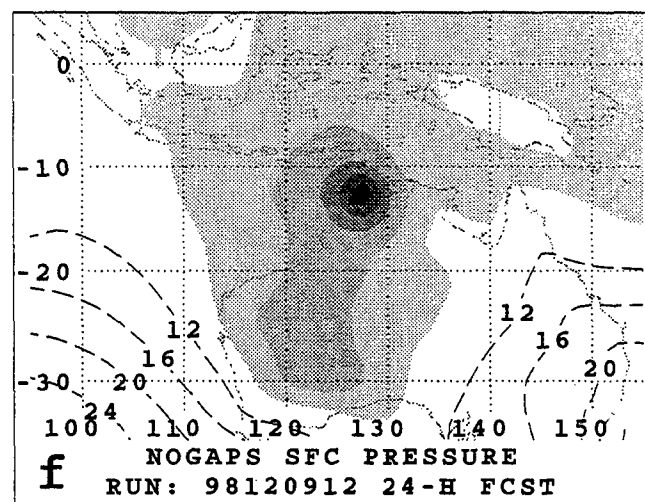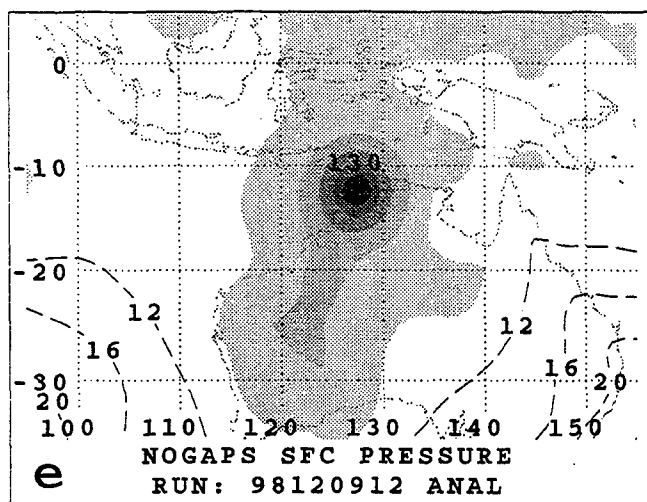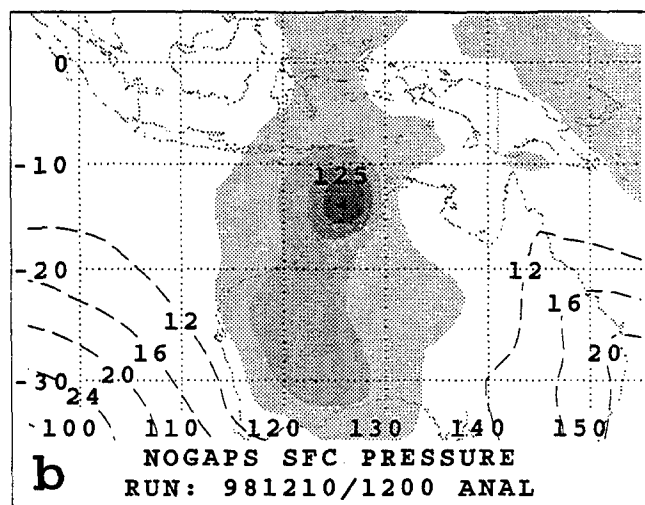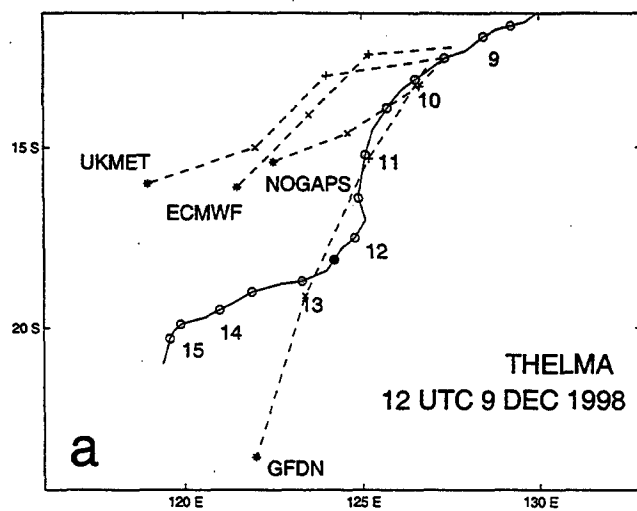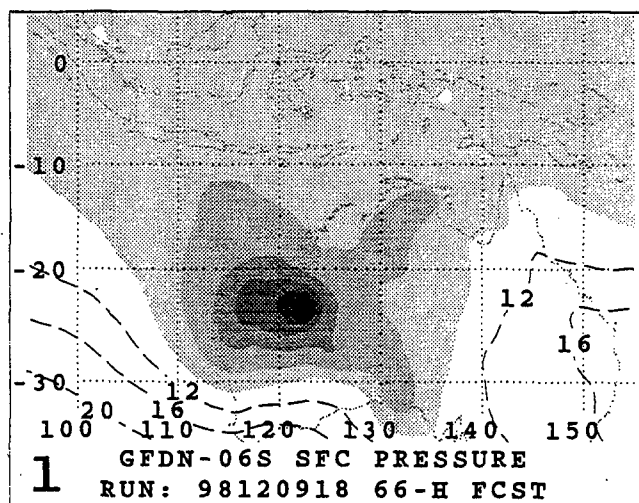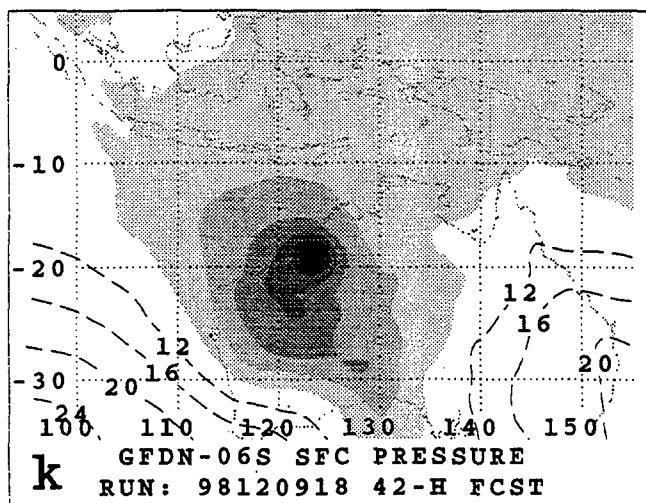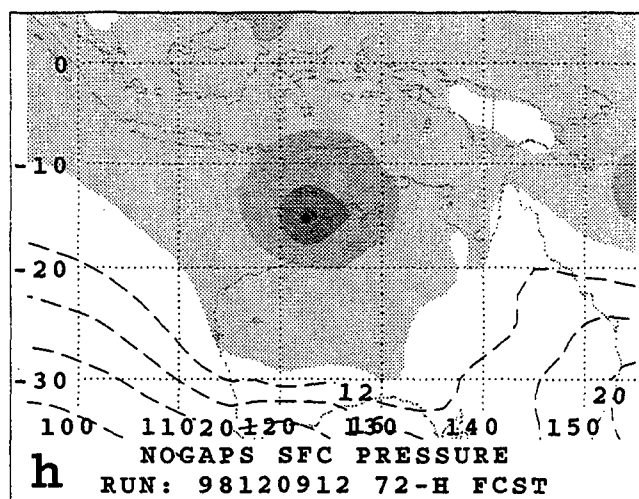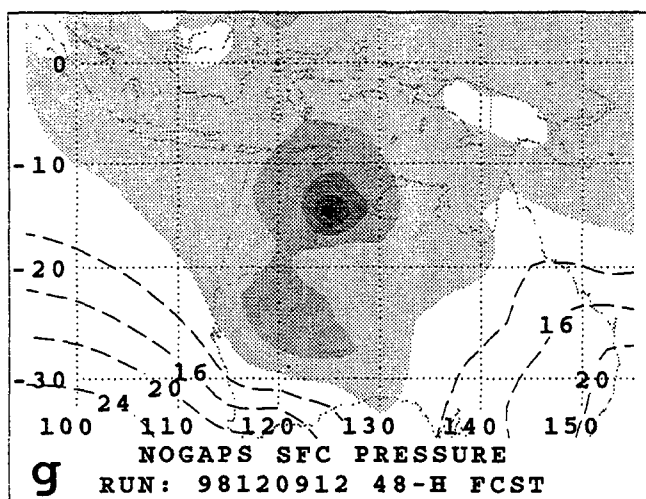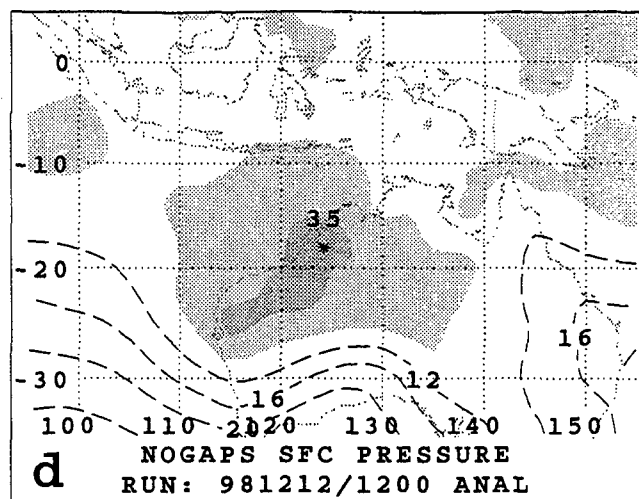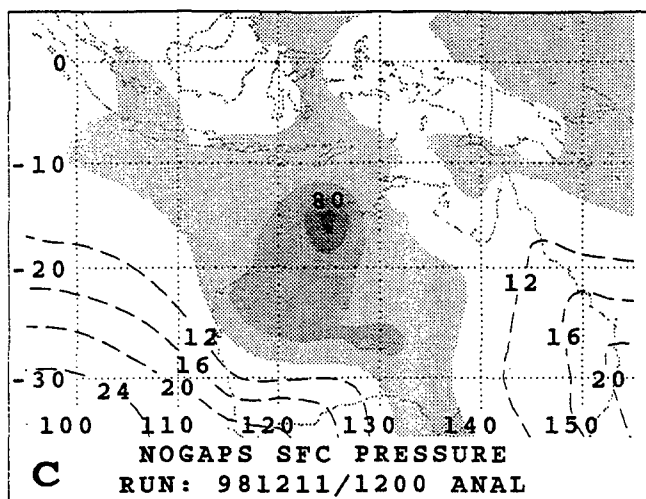since it is only in the immediate region of the TC that the GFDL spin-up vortex replaces the NOGAPS representation of the vortex. Notice that Thelma is embedded in an extensive trough that extends from northwest to southeast, where the trough "breaks" the subtropical anticyclone. Another key feature at the initial time is the midlatitude trough that is progressing eastward across 100°E.

By 24 h, TC Thelma has translated southwestward along the Northwest Australia coast (Fig. 3.2b), and the subtropical anticyclone poleward of Thelma has weakened as the midlatitude trough has approached and deepened off the Western Australia coast. This evolution has been predicted well by both the NOGAPS (Fig. 3.2f) and GFDN (Fig. 3.2j) models.

By 48 h, Thelma has just crossed the Northwest Australia coast (Fig. 3.2c). The large cyclonic circulation of Thelma and the weakened midlatitude trough along the Western Australia coast have compressed the subtropical anticyclone between them, but a thin ridge remains to the southwest of Thelma. The NOGAPS 48-h forecast (Fig. 3.2g) is generally correct, although the translation speed for Thelma is slow. Although the midlatitude trough is forecast too deep, a clear subtropical anticyclone remains between the trough and Thelma. In the GFDN model (Fig. 3.2k), the poleward translation speed for Thelma is too large so that the storm is already ashore. Nevertheless, the intensity remains high and an extensive cyclonic circulation has nearly connected with the midlatitude trough, which is predicted by the GFDL model to be even stronger than in the NOGAPS model. That is, the GFDL model is predicting an extratropical cyclogenesis, and the deepening cyclonic circulation is contributing to an accelerated poleward flow over Thelma to the east of the trough.

By 72 h, Thelma has filled rapidly to an intensity of only 35 kt as it has moved slowly inland (Fig. 3.2d). Only a weak cyclonic trough remains off the West Australia coast, with a broader and better defined subtropical anticyclone re-established between the trough and Thelma compared to 24 h previously (Fig. 3.2c). In the 72-h NOGAPS forecast (Fig. 3.2h), the offshore cyclonic trough did not extend equatorward and the intervening anticyclone was thus too strong. Consequently, a more equatorward steering flow (notice the isotach maximum to the southwest) was forecast over Thelma, which is thus forecast to still be offshore. In the GFDN 72-h forecast (Fig. 3.2l), a vigorous cyclonic circulation remains even though the Thelma remnants have penetrated far poleward over land. Whereas the analysis (Fig. 3.2d) has an intervening anticyclone, the Thelma remnants have approached the midlatitude trough so that no anticyclone exists between them. The suggestion is clearly that the Thelma remnants have been "captured" by the trough circulation, which accounts for the poleward track error with a magnitude of 405 n mi at 72 h. In this sense, some contribution to the 48-72 h error may be from the Excessive Baroclinic Cyclone Interaction (E-BCI) error mechanism to be described in Chap. 3g. This multiple error mechanism situation may make attribution of the more dominant mechanism somewhat difficult. For the forecaster, clear identification of either error mechanism would be justification for eliminating that model track.

Additional evidence of the E-MCG for the GFDN track forecast of TC Thelma may be found in the sea-level pressure (SLP) prediction in Fig. 3.3j-l. Whereas Thelma is quite intense and just offshore at the initial time (1200 UTC for NOGAPS in Fig. 3.3e and 1800 UTC for GFDN in Fig. 3.3i), both analyses have a concentrated SLP signature at the equatorward end of a

trough of low SLPs over Western Australia. Notice that this trough is about 4 mb deeper in the NOGAPS analysis than in the GFDN analysis. By 24 h, the NOGAPS forecast (Fig. 3.3f) reflects well the corresponding analysis (Fig. 3.3b). The GFDN forecast (Fig. 3.3j) already has evidence of the approaching trough with a 996 mb trough along 120°E. Again at 48 h, the NOGAPS forecast (Fig. 3.3g) resembles well the corresponding analysis (Fig. 3.3c), except that the SLP center of Thelma trails the verifying position. In addition to maintaining too strong of a center for Thelma over land at 48 h, the GFDN forecast (Fig. 3.3k) has a vigorous SLP trough oriented northwest-southeast adjacent to Thelma, which is consistent with the 500-mb trough in Fig. 3.2k. Finally, the SLP center associated with the Thelma remnants in the 72-h GFDN forecast (Fig. 3.3l) have been rapidly translated poleward to form an east-west trough along 23°S in conjunction with the midlatitude trough. Thus, both the intensity and the pattern of the GFDN SLP forecast differ greatly from the verifying analysis (Fig. 3.3d) or NOGAPS 72-h forecast (Fig. 3.3h).

With the benefit of hindsight in the retrospective analysis of large track errors, it is known that it is the GFDN forecast that is in error, and the NOGAPS forecast is the more nearly correct forecast scenario (albeit slow). The forecaster would not know in real-time which of these two plausible scenarios was the more likely to be correct, although the rapid translation speed and intense SLP feature in the 48- and 72-h GFDN forecasts would raise suspicions. For the western North Pacific (Table 2.1), the E-MCG is a frequently occurring error mechanism, whereas an insufficient (I-MCG) is not listed as a frequently occurring error mechanism for NOGAPS (or any other of the four models). As Carr and Elsberry (2000b) point out, E-MCG in a GFDN forecast was typically accompanied by a E-MCG in the NOGAPS forecast, although not with sufficient severity to cause a 72-h error greater than 300 n mi. However, this study of Southern Hemisphere errors (Table 2.2) suggests that I-MCG can occur for the NOGAPS (and UKMO) forecasts. Thus, the distribution of frequently occurring error sources does not provide as clear guidance in this Southern Hemisphere case as it would be if the western North Pacific forecaster faced an E-MCG choice for GFDN versus the I-MCG choice for NOGAPS.

c.   *Case study of Insufficient-Midlatitude Cyclogenesis (I-MCG)*

As indicated in Table 2.2, the NOGAPS and UKMO models had I-MCG errors in about 10% and 13% of their forecasts in this sample. The case of TC Susan is an example in which both models had an I-MCG error. At 1200 UTC 5 January 1998, Susan had been moving slowly poleward (Fig. 3.4a) in the Standard/Poleward Flow pattern/region (see Appendix for definition) and approaching the subtropical ridge axis. All of the four models predict a rapid acceleration to the southeast. Whereas the GFDN and ECMWF model guidance is excellent for this difficult forecast scenario, the NOGAPS and UKMO forecasts are slow and to the right.

Another difficult aspect of this forecast is that TC Susan (near 14°S, 170°E) has another TC to the west near 16°S, 156°E and a monsoon trough circulation to the east near 13°S, 176°W (Fig. 3.4e). The ECMWF initial analysis (Fig. 3.4i) has similar circulations, but the subtropical anticyclone to the south is somewhat weaker and the midlatitude troughs appear to have more amplitude than in the UKMO analysis. In particular, a short-wave trough off the east coast of Australia has more amplitude.
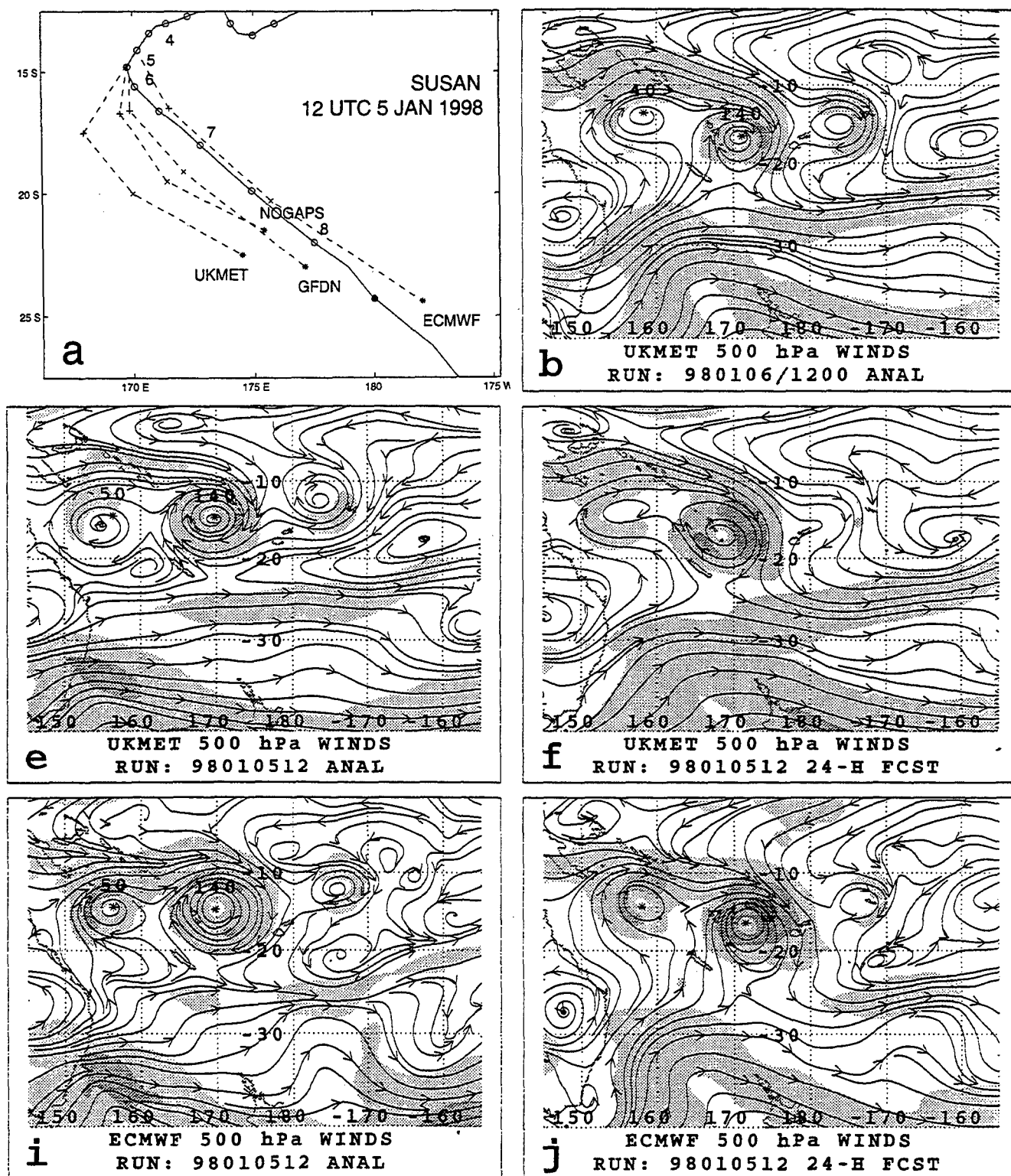
Fig. 3.4. Tracks (panel a) and 500-mb streamline/isotach analysis (panels b-d) and UKMO (panels f-h) and ECMWF (panels j-l) forecasts as in Fig. 3.2, except for TC Susan beginning at 1200 UTC 5 January 1998.

20

c UKMET 500 hPa WINDS
RUN: 980107/1200 ANAL

d UKMET 500 hPa WINDS
RUN: 980108/1200 ANAL

g UKMET 500 hPa WINDS
RUN: 98010512 48-H FCST

h UKMET 500 hPa WINDS
RUN: 98010512 72-H FCST

k ECMWF 500 hPa WINDS
RUN: 98010512 48-H FCST

l ECMWF 500 hPa WINDS
RUN: 98010512 72-H FCST

Fig. 3.4. (continued)

21
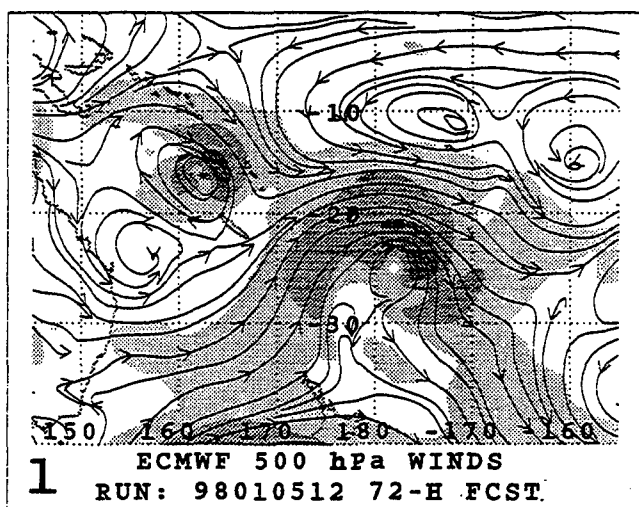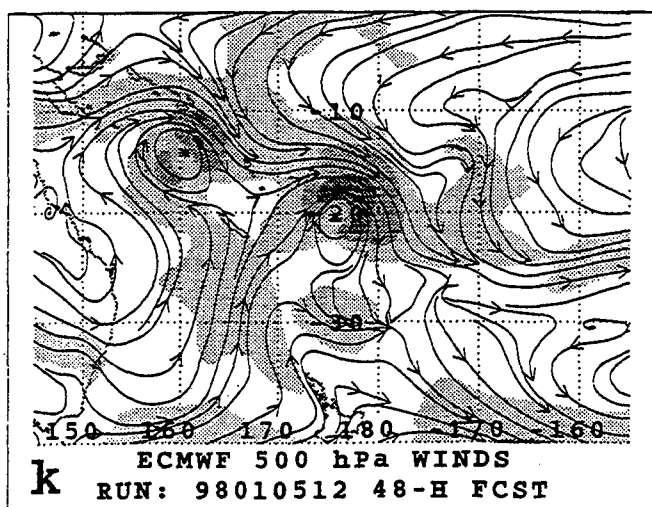
By 24 h, Susan has moved poleward and the approach of a high amplitude midlatitude trough toward Susan is evident in the UKMO analysis (Fig. 3.4b). This trough has further broken the subtropical anticyclone. By contrast, the UKMO 24-h forecast (Fig. 3.4f) still has a weak ridge poleward of Susan, perhaps because the amplitude of the midlatitude trough is underpredicted. Although the ECMWF 24-h forecast (Fig. 3.4j) has a better representation of the midlatitude trough than the UKMO model, the amplitude is a little under-predicted.

By 48 h, the high amplitude midlatitude trough has deepened significantly as it approaches TC Susan (Fig. 3.4c). The associated steering flow east of the trough has contributed to the rapid translation of Susan toward the southeast at 1200 UTC 7 January (Fig. 3.4a). Because the amplification (cyclogenesis) of the midlatitude trough is under-forecast at 48 h by the UKMO model (Fig. 3.4g), the trough has not "captured" the TC to an adequate extent. Whereas the stronger isotach maximum is to the northeast of Susan in the UKMO forecast, another maximum exceeding 20 kt to the west of Susan implies that the southerly flow on that side is impeding the poleward translation of Susan. In the ECMWF 48-h forecast (Fig. 3.4k), the midlatitude trough amplitude and the "capture" of the TC by the trough are better predicted than in the UKMO model. Consequently, the ECMWF 48-h forecast position is farther east and poleward than the UKMO position (Fig. 3.4a).

At 72 h, the high amplitude midlatitude trough has captured the TC, which still has an intensity of 90 kt, and the combined circulation is accelerating to the southeast (Fig. 3.4d). The UKMO 72-h forecast (Fig. 3.4h) has under-predicted the midlatitude trough amplitude and the TC position is too far to the west. The ECMWF 72-h forecast (Fig. 3.4l) has more correctly predicted the amplitude and position of the midlatitude trough and its coupling with the TC circulation. If anything, the ECMWF model has over-forecast the strength of the winds around the trough and TC compared to the UKMO analysis (Fig. 3.4d). However, the UKMO analysis may also be an under-representation if the first-guess from the previous UKMO short-term forecast is a more important contributor than actual observations to the analysis.

Given the difficulty of forecasting such rapid acceleration of TCs into the midlatitude westerlies, the guidance from the four dynamical models is not that bad. Certainly the likely path is relatively well defined by the guidance, and the question for the forecaster would be the translation speed. Knowing the UKMO and NOGAPS have a tendency toward I-MCG (Table 2.2), the forecaster may be advised to go with the ECMWF and GFDN tracks in this case.

d.   Case study of Excessive-Midlatitude Anticyclogenesis (E-MAG)

Whereas the E-MCG error mechanism can lead to dramatic shifts from a zonal to a meridional environmental flow around the TC, more subtle shifts to a more zonal flow poleward of the TC can occur that may then cause significant track errors. The case of TC Elsie is a case of E-MAG that contributed a westward deflection of the UKMO and NOGAPS tracks (Fig. 3.5a).

At 0000 UTC 13 March 1998, TC Elsie was a 90-kt storm equatorward of the subtropical anticyclone (Fig. 3.5b). Owing to the strength of the eastern subtropical anticyclone cell, and the peripheral anticyclone to the northeast, the track of Elsie also has a poleward component (Fig.
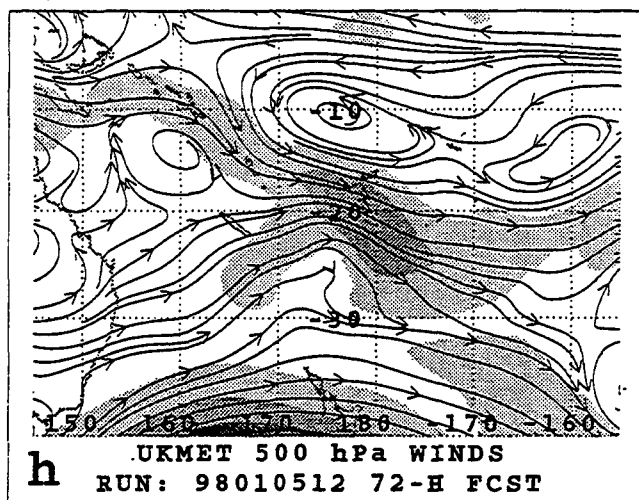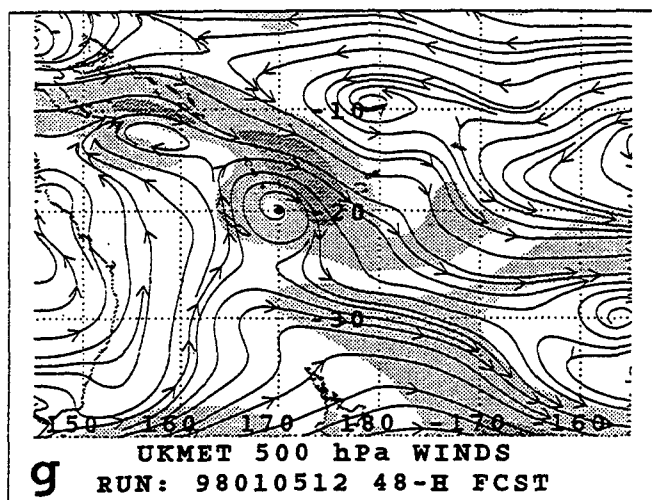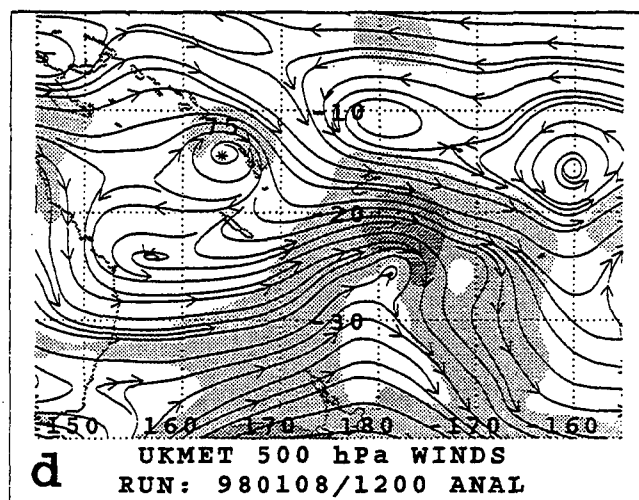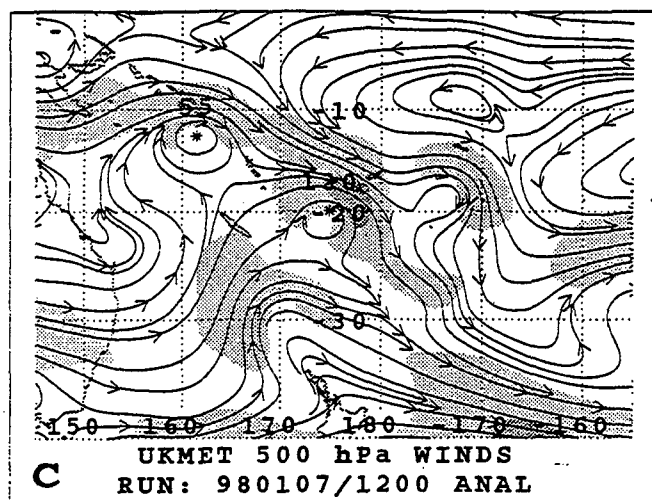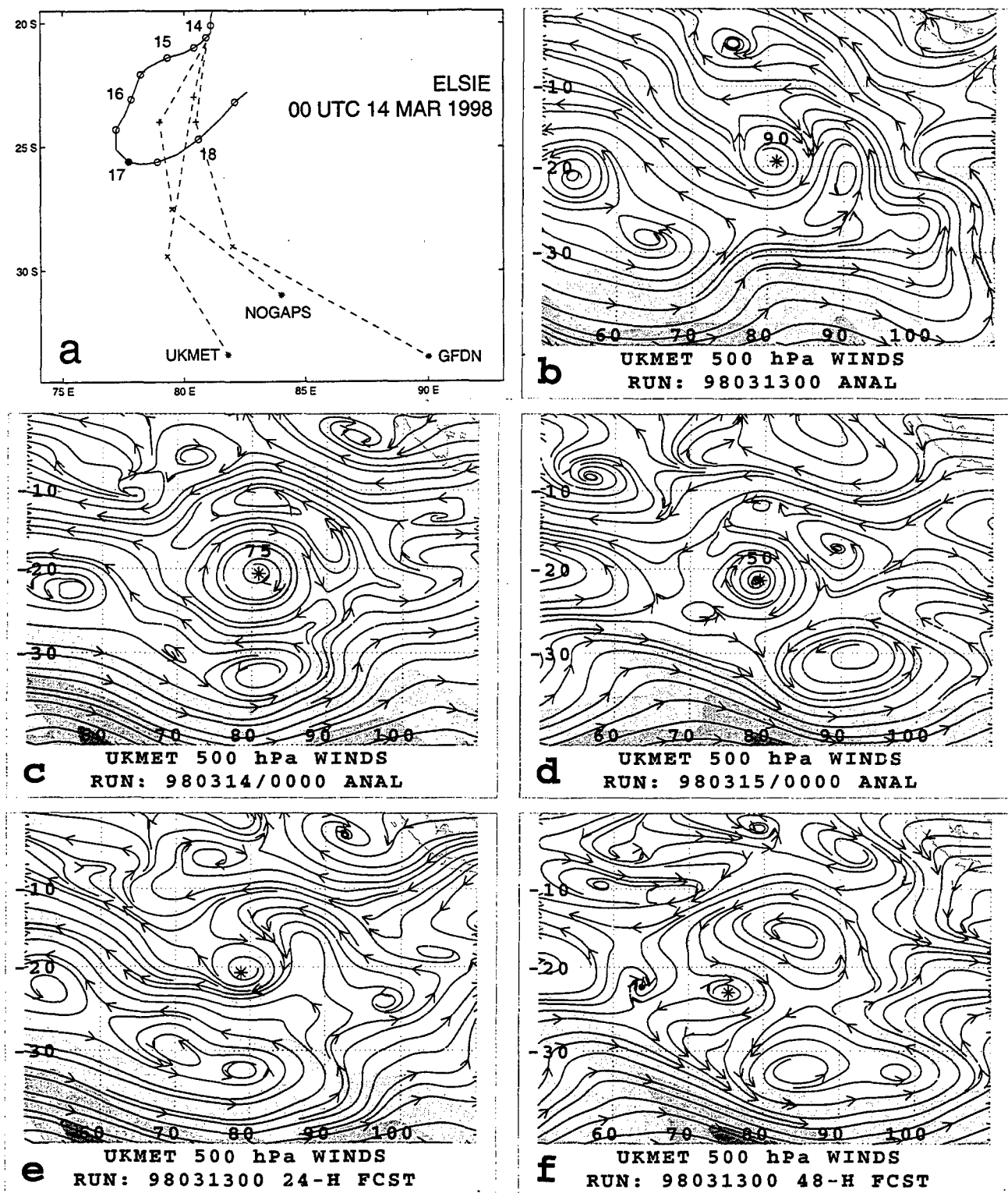
Fig. 3.5 Tracks (panel a) and 500-mb streamline/isotach analyses (panels b, c, and d) at the initial time and 24 h and 48 h and the 24-h and 48-h UKMO forecasts (panels e and f) as in Fig. 3.2, except for TC Elsie beginning at 0000 UTC 13 March 1998.

23

3.5a). By 24 h, the subtropical anticyclone on the south (east) side has strengthened (weakened) as the midlatitude ridge has moved eastward (Fig. 3.5c). However, the UKMO 24-h forecast (Fig. 3.5e) has over-predicted the amplitude of the subtropical anticyclone, especially the cell near 30°S, 70°E to the southwest of Elsie. As a consequence, a more westward steering flow over Elsie is predicted, which is also reflected by the shift of the isotach maximum more to the south of Elsie compared to the east side 24 h previously.

At 48 h, Elsie is moving only slowly westward (Fig. 3.5a) as it is within a ring of anticyclonic circulations (Fig. 3.5d) without a well-defined steering current. However, the UKMO 48-h forecast (Fig. 3.5f) has a subtropical anticyclone cell more to the south-southeast (versus southeast) of Elsie and a stronger ridge to the southwest of Elsie than are present in the analysis (Fig. 3.5d). Thus, the E-MAG in the UKMO model has led to a persistent westward bias (Fig. 3.5a), which is expected from the conceptual model (Fig. 3.1). However, the continued poleward translation of Elsie departs from the MAG conceptual model (TC C in panel c → panel d in Fig. 3.1). This poleward displacement is related to the growing peripheral anticyclone in this case and the asymmetry in the eastern and western subtropical anticyclone cells compared to the symmetric cells in the conceptual model. That is, the conceptual model must be considered to be a flexible template that is adjusted for such asymmetries.

By 72 h (not shown), E-RVS becomes a more dominant error mechanism than E-MAG, and Elsie eventually reverses direction (Fig. 3.5a) as the steering level is shifted to a lower level in the troposphere.

The key feature in this case is the intensification of the subtropical anticyclone poleward of Elsie. This change is in part due to the eastward translation of the midlatitude ridge such that it phases with the subtropical ridge. A contribution to the strengthening of the subtropical anticyclone to the southwest of Elsie may also be due to a Rossby wave train. That is, the approach of a midlatitude trough from the southwest may lead to this anticyclone enhancement, a cyclonic spinup around the Elsie circulation, and then an amplification of the anticyclone to the northeast of Elsie by 48 h in the UKMO forecast (Fig. 3.5f).

As indicated above, the changes in the subtropical anticyclone cells during E-MAG may be relatively subtle compared to an E-MCG case in which a vigorous midlatitude cyclone develops with an easily identifiable signature in the satellite imagery. The key point for the forecaster is that a broad view of TC environmental changes includes midlatitude effects as well as tropical region effects.

e.   *Description of Excessive-Response to Vertical wind Shear (E-RVS)*

Conceptual models of Excessive and Insufficient RVS are given in Fig. 3.6. It is assumed that a significant difference in the vertical depth and the associated intensity exists between the actual TC and the model-predicted TC in the presence of a vertically-sheared environmental flow (Fig. 3.6d), so that the model representation of the TC will have a different translation speed (Fig. 3.6c). Typically, the difference between the actual and model-depicted vertical structure of the TC tends to become greater with increasing forecast interval (Fig. 3.6d), which results in increasing differences in translation speeds, and thus TC track errors (Fig. 3.6c). *Insufficient* RVS (I-RVS) is said to be occurring if the model-depicted vertical structure of the
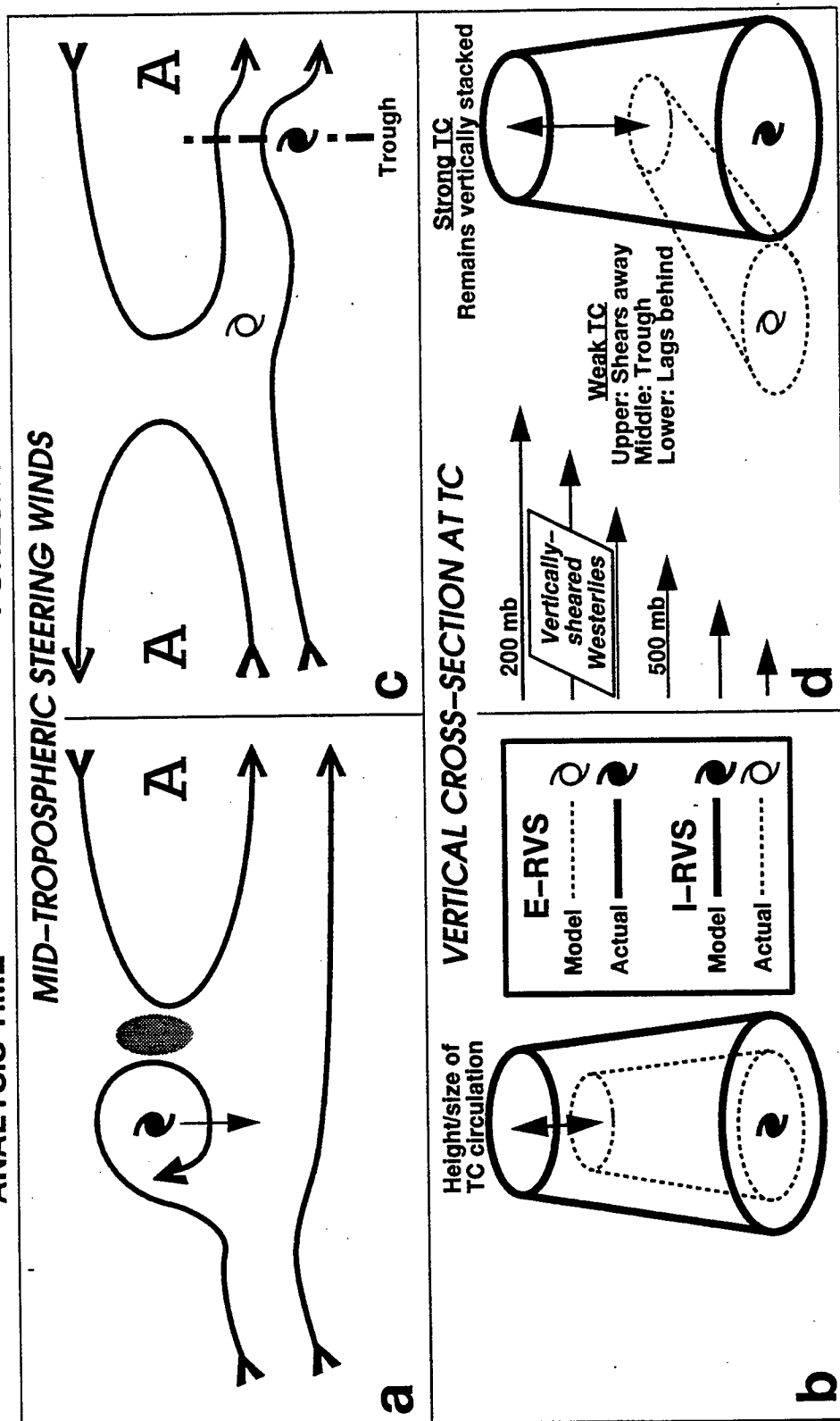
Fig. 3.6 Conceptual model as in Fig. 3.1, except for the Response to Vertical wind Shear (RVS) of a TC in a dynamical model. (a) Plan view of the 500 mb environmental flow and (b) vertical cross-section along the vertical wind shear vector through the TC with different vertical (and presumably horizontal) extents in the model and in nature at analysis time. (c-d) Corresponding plan view and vertical cross-section at verification time in which excessive RVS (E-RVS) causes the vortex to be too shallow (panel d, dotted) and the track to have a slow bias (panel c, dotted). Insufficient RVS (I-RVS) leads to a vortex that is too deep and a fast track bias (dashed lines in panels c and d).

TC is too deep and upright (i.e., not tilted) compared to reality, which will result in a track forecast that is too fast (Fig. 3.6b). Conversely, *Excessive* RVS (E-RVS) is said to be occurring if the model-depicted vertical structure of the TC is too shallow and excessively tilted, which will result in a track forecast that is too slow.

Although the depictions of the RVS contain some basic similarities to the MSE conceptual model (e.g., compare TC labeled B in Fig. 3.1a with Fig. 3.6a), the two situations are fundamentally different with regard to the response of the TC structure to the environmental flow. The RVS mechanism is invoked in situations in which differences in the TC structural response to environmental vertical wind shear best explain forecast track differences. The four MSE mechanisms in Fig. 3.1 are applied when significant differences in environmental steering, which are not essentially related to the presence of the TC and do not result in TC vertical structure differences, seem to best explain differences in the forecast track.

The predominant tendency for RVS to contribute to large track errors (Table 2.2) is for E-RVS for the three global models, with about 18%, 13%, and 11% for the NOGAPS, UKMO, and EXMWF errors, respectively. No cases of I-RVS were recorded for these three global models. Conversely, only the (regional) GFDN model has cases (~ 4%) of I-RVS, and had no cases of E-RVS. The physical explanation for the I-RVS in the GFDN model is that its small horizontal spacing (~ 18 km) on the inner nested grid allows an intense vortex to be maintained, which may be able to resist (to too great of an extent in some cases) the degrading effects of vertical wind shear. By contrast, the global models with horizontal grid sizes of 50-75 km do not resolve the inner structure of high winds, and may be too susceptible to vertical wind shear effects

A thorough analysis of either the real or the model TC circulation vertical wind shear would require a time-consuming evaluation of multiple levels and cross-sections through both the real and model TC. Such an analysis of the model TC might be difficult to accomplish under the time constraints of operational TC forecasting, and the forecaster does not have access to full-resolution model fields that would better reveal the structure of the TC in the model. In addition, observations of the TC structure are not available in the Southern Hemisphere owing to the lack of aircraft reconnaissance. Thus, it is proposed that an expedient means to infer RVS-induced changes in the vertical structure of the TC is to compare the sea-level pressure forecasts. Assuming hydrostatic equilibrium and thermal wind balance, a positive correlation may be expected between the vertically integrated wind strength and the minimum sea-level pressure of the model TC. This correlation is represented in Fig. 3.6b and d in that the TC circulation with less vertical extent has a smaller sea-level pressure pattern (dotted) compared to the TC circulation with more vertical extent (dashed).

Another potential indicator of E-RVS for a large global model 72-h error is that the trough that represents the 500-mb circulation of the TC becomes noticeably displaced down-shear of the low-level center in the 48- to 72-h forecast fields. When the 500-mb circulation and low-level centers remain closely aligned throughout the forecast period (and no other error mechanism is operative), the global model track forecast may be reasonably accurate. Carr and Elsberry (2000 b) indicate that the increasing downshear displacement between the 500 mb and low-level centers at 48 h and 72 h is often an indication of increasing along-track (slow) error magnitude. That is, a TC embedded in strong (but nearly uni-directional) midlatitude vertical

wind shear that is predicted to have an E-RVS will be too shallow and thus will have a steering flow over a shallower depth. Thus, the predicted motion is slower than for the actual TC, but will be in the same general direction. Another scenario is that the "shearing off" of the upper warm core of the model vortex will leave only a low-level vortex that is in a trade-wind steering flow with a quite different direction from the deep tropospheric steering that previously applied.

f.   Case study of Excessive-Response to Vertical wind Shear (E-RVS)

At the initial time (1200 UTC 7 October 1998), TC Zelia is translating southeastward in a Poleward/Poleward Flow (P/PF) pattern/region (see Appendix) with an isotach maximum on the northeast side (Fig. 3.7e). Over the 72-h period, the translation of Zelia slows, turns northeastward, and then reverses direction to move northwestward (Fig. 3.7a) It is generally accepted that weak storms such as Zelia are more susceptible to vertical wind shear than are intense TCs. The issue here is how well do the models predict this shear effect on the vortex vertical structure, and thus on the steering current of the storm (Fig. 3.6).

After 24 h, Zelia has increased in intensity to 45 kt and the 500-mb trough is essentially above the surface position (asterisk in Fig. 3.7b). However, a separation between the open 500-mb trough and the surface position is already evident in the UKMO 24-h forecast (Fig. 3.7f). The UKMO forecast, which has moved the storm to the south with an imminent west turn, is already in error by 127 n mi by 24 h. Beginning from a noisy initial analysis without a well-defined vertical structure (Fig. 3.7i), the ECMWF 24-h forecast (Fig. 3.7j) also has only a weak 500-mb trough that is southeast of the surface center. As shown in Fig. 3.7a, the ECMWF forecast track is toward the northwest, and the 24-h track error is already 248 n mi.

In the 48-h analysis (Fig. 3.7c), Zelia is clearly in the southeastward flow ahead of an upper-level trough, but the 500-mb trough and surface center are still vertically aligned. However, the UKMO 48-h forecast (Fig. 3.7g) has southwestward flow directly over the surface center with a clear separation from the 500-mb trough. The UKMO westward track at 48 h (Fig. 3.7a) indicates a decoupling of the vortex, which is clearly not moving with the 500-mb flow, but with a lower tropospheric steering flow. Similarly, the ECMWF 48-h forecast has no indication of the vortex, which is moving northwestward (Fig. 3.7a). These trends in the UKMO and ECMWF model forecasts continue at 72 h (Figs. 3..7h and 3.l), and the track errors continue to grow (Fig. 3.7a).

The guidance to the forecaster from Table 2.2 is that the global models are most likely to experience E-RVS, which will lead to a slow along-track forecast if the lower-tropospheric vortex becomes decoupled too early from the upper-troposphere warm core as in the conceptual model (Fig. 3.6). Thus, the vortex remnants move in the direction and with the speed of a lower-tropospheric steering flow. By contrast, the high resolution (regional) GFDL model experienced only I-RVS, which tends to result in a too fast track as the vortex remains vertically coherent and thus has a deep tropospheric steering flow that includes the high wind speed aloft that creates the vertical wind shear.
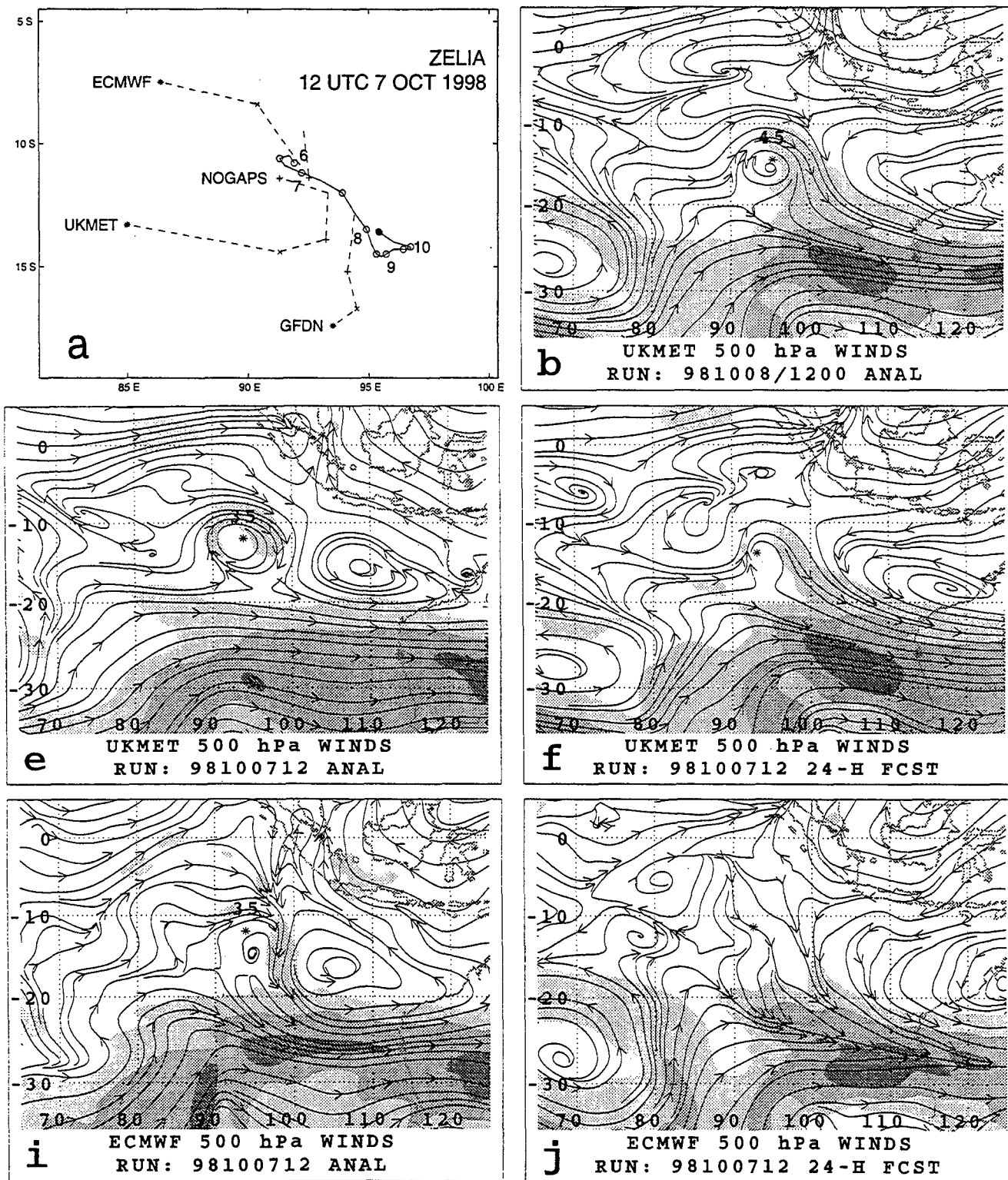
Fig. 3.7. Tracks (panel a) and 500-mb streamline/isotach analyses (panels b-d) and UKMO (panels f-h) and ECMWF (panels j-l) forecasts as in Fig. 3.2, except for TC Zelia beginning at 1200 UTC 7 October 1998.

c UKMET 500 hPa WINDS
RUN: 981009/1200 ANAL

d UKMET 500 hPa WINDS
RUN: 981010/1200 ANAL

g UKMET 500 hPa WINDS
RUN: 98100712 48-H FCST

h UKMET 500 hPa WINDS
RUN: 98100712 72-H FCST

k ECMWF 500 hPa WINDS
RUN: 98100712 48-H FCST

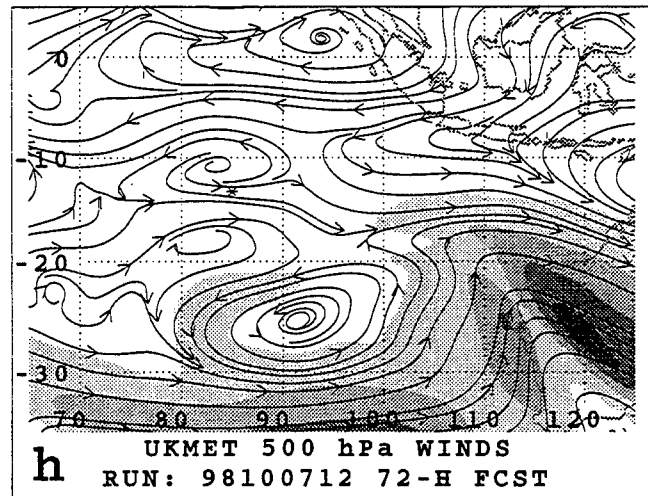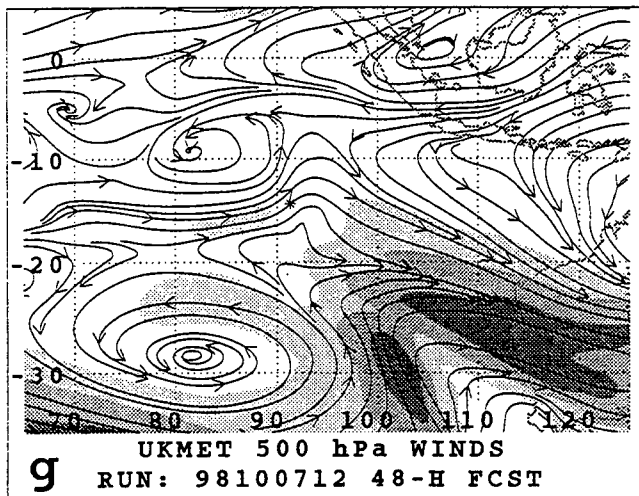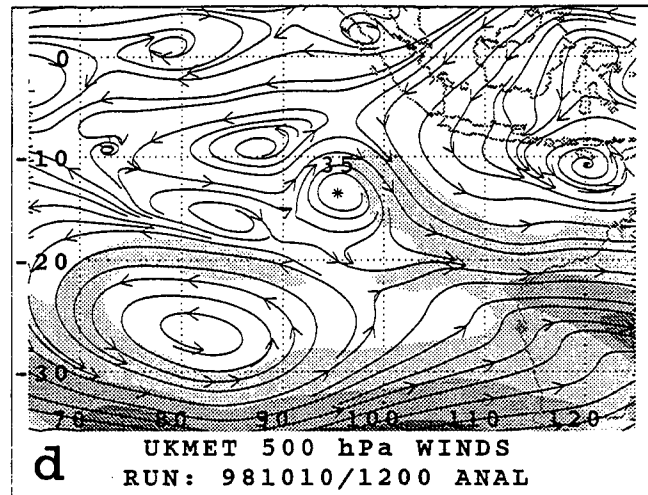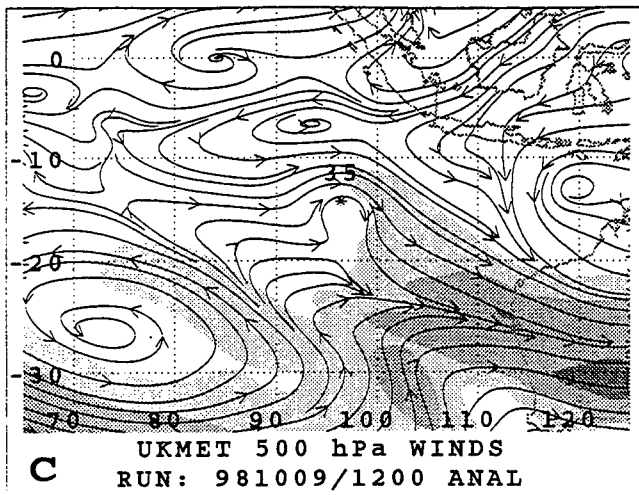l ECMWF 500 hPa WINDS
RUN: 98100712 72-H FCST
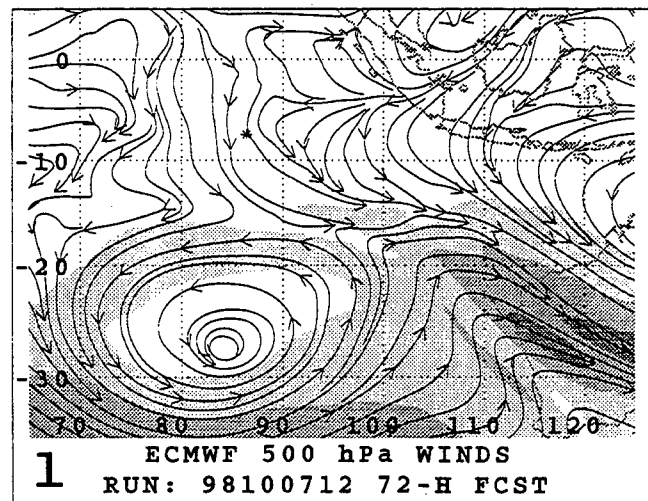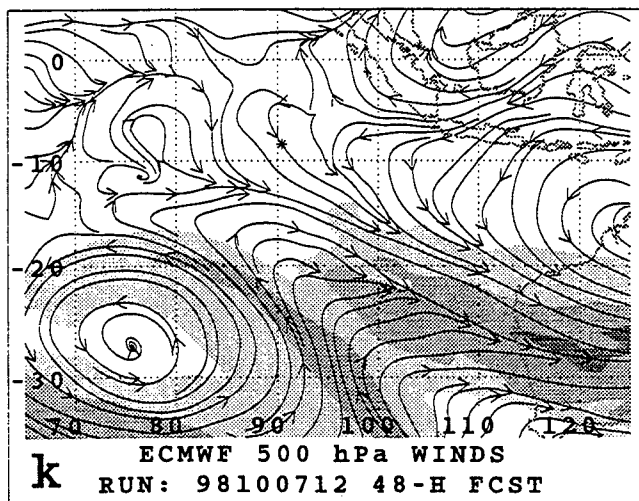
Fig. 3.7 (continued)

g. Description of Baroclinic Cyclone Interaction (BCI)

Erroneous Baroclinic Cyclone Interaction (BCI) in the dynamical model is said to occur when extratropical transition is either over- or under-predicted such that a significant TC track error results (Fig. 3.8). In a potential extratropical transition scenario, the TC is in the vicinity of the mid-tropospheric subtropical ridge axis with a midlatitude trough to the south or southwest, and an upper-tropospheric jet maximum is to the southeast (or perhaps southwest) of the TC (Fig. 3.8a). The equatorward entrance (or poleward exit) region of the jet maximum has an enhanced upper-tropospheric divergence that tends to produce corresponding areas of lower-tropospheric convergence and cyclogenesis that may appear to accelerate the TC southeastward toward the location of maximum cyclogenetic tendency (Fig. 3.8b). Concurrently, poleward (equatorward) flow on the east (west) side of the TC in the presence of a large-scale meridional temperature gradient results in warm (cold) temperature advection (Fig. 3.8b) that may amplify the upper-level trough/ridge pattern via a process called self-amplification (Fig. 3.8c). To the extent that the TC becomes constructively aligned with a midlatitude area of baroclinic cyclogenesis, significant deepening occurs and the TC undergoing extratropical transition develops frontal characteristics (Fig. 3.8d). Since the lower-tropospheric warm and cold temperature advection (Fig. 3.8b) affects the structure of the mid-tropospheric winds that steer the TC, a vigorous BCI event may have a significant impact on the TC track (Fig. 3.8d; see arrows). Typically, the greater the deepening of the TC that is undergoing extratropical transition, the more poleward will be the track owing to the BCI-induced amplification of the mid-tropospheric ridge to the southeast of the TC. However, the BCI process can result in various combinations of direction and speed changes depending on the tilt of the midlatitude trough and the orientation of the midlatitude trough relative to the TC. *Excessive* BCI (E-BCI) is said to occur when the extratropical transition process occurs more vigorously (or falsely) in the model compared to reality. Conversely, Insufficient BCI (I-BCI) is considered to occur when the extratropical transition process occurs less vigorously (or not at all) in the model compared to reality.

At least for this sample of Southern Hemisphere TCs (Table 2.1), the BCI error mechanism seems to be less frequent (22 of 241) than Carr and Elsberry (2000b) found for the western North Pacific (33 of 198), where this error mechanism was the second-most frequent. In particular, the NOGAPS and GFDN forecasts in the Southern Hemisphere did not seem to be affected (Table 2.2) nearly as much as in the western North Pacific. The models most affected in this study are the UKMO with about 11% I-BCI and the ECMWF with about 11% E-BCI. Whether these dynamical model track error differences for Southern Hemisphere TCs are due to the relatively small sample sizes will have to be determined later from larger samples.

One experience from this study is that multiple midlatitude error sources may contribute to the large track errors. For example, an excessive or insufficient RVS event may precede the period of erroneous BCI such that the slow or fast track caused by the RVS then contributes to the severity of the erroneous BCI. This connection between RVS and BCI is to be expected since the baroclinity of the midlatitude environment that enables baroclinic development is also associated with vertical wind shear. In addition, track errors caused by one of the four Midlatitude System Evolutions (MSE) in Fig. 3.1 may lead to a situation that then contributed to erroneous BCI. Given the dominance of the MSE mechanisms in the Southern Hemisphere

Baroclinic Cyclone Interaction (BCI) Error Mechanism

ANALYSIS TIME

MID-TROPOSPHERIC STEERING WINDS

a

LOWER-TROPOSPHERIC HEIGHTS

Cold Advection

Warm Advection

L

Maximum cyclogenesis area under jet left entrance region

TC drawn toward cyclogenesis area and enhances cyclogenesis by amplifying upper-level trough via warm/cold advection

b

FORECAST VERIFYING TIME

Jet Maxima:
Remain separate (I-BCI)
Connect (E-BCI)

A

Midlatitude amplitudes are too:
Low (I-BCI)
High (E-BCI)

c

I-BCI
Too slow
Too small
Too shallow

E-BCI
Too fast
Too large
Too deep

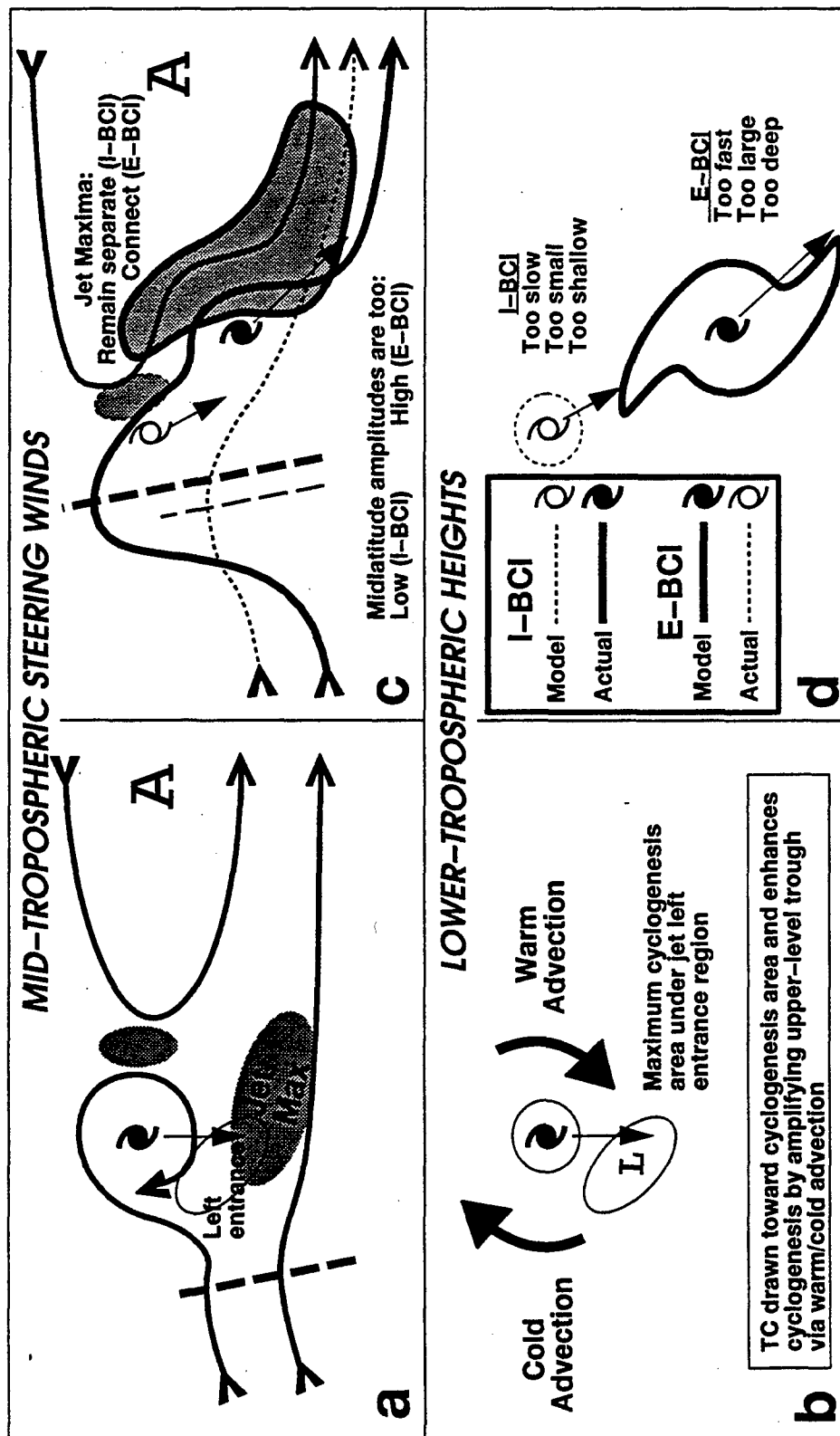I-BCI
Model
Actual

E-BCI
Model
Actual

d

Fig. 3.8 Schematics of two stages of Baroclinic Cyclone Interaction with a recurving TC that is potentially undergoing extratropical transition. If the midlatitude trough amplifies (solid lines in panel c) to enhance the poleward steering current over the TC, the jet maximum and isotach maximum to the east of the TC will connect. If the midlatitude trough does not amplify, these features will not connect. Modifications in the lower tropospheric thermal structure (panels b and d) lead to changes in the environmental steering of the TC (panel c). *Excessive* BIC usually results in a more poleward track bias and *insufficient* BCI results in a slow track bias (panel d).

31

(Table 2.2), it may be that incorrect forecasts of the high-amplitude midlatitude trough and ridge circulation evolutions are simply more important contributors to large TC track errors than are the BCI error sources.

For this retrospective study, the error mechanism that is judged to have most contributed to the large track error is selected. For the forecaster in real-time situations, which of the multiple error sources most contributed to anomalous track forecast is not so important, since the objective is to reject any track for which good evidence exists that it is likely to be erroneous.

h.   *Case study of Baroclinic Cyclone Interaction (BCI)*

The dynamical model forecasts for TC Anacelle from 1200 UTC (1800 UTC for GFDN) 11 February 1998 provide examples of I-BCI for the UKMO and ECMWF models and E-BCI for the NOGAPS and GFDN models. Although the UKMO and ECMWF tracks (Fig. 3.9a) are oriented along the storm track, they are slow as the rapid poleward acceleration of the TC remnants is underforecast. Both the NOGAPS and GFDN tracks have approximately the correct length, but the E-BCI has led to a poleward displacement as in the conceptual model (Fig. 3.8).

At 1200 UTC 11 February, Anacelle is near 21°S, 60°E and has an intensity of 115 kt (Fig. 3.9e). A broad midlatitude trough is approaching, with an intense jet streak to the southeast. Notice the similarity between this NOGAPS analysis and the corresponding ECMWF analysis (Fig. 3.9i), including a pronounced short-wave trough to the west of Anacelle at about 25°S, 46°E.

By 24 h, the midlatitude trough and TC Anacelle are clearly interacting (Fig. 3.9b). Whereas the ECMWF 24-h forecast (Fig. 3.9j) has a broader trough along 30°S, the NOGAPS 24-h forecast (Fig. 3.9f) has embedded the compact Anacelle circulation into the midlatitude trough. However, the difference in the forecast positions is small at 24 h (Fig. 3.9a).

By 48 h, the NOGAPS analysis (Fig. 3.9c) has a complex structure near and to the southeast of Anacelle as another short-wave trough is approaching from the west. The ECMWF 48-h forecast (Fig. 3.9k) has apparently put the TC at an intermediate position between the real TC position and the short wave to the west, and thus is too far west (Fig. 3.9a). As at 24 h, the NOGAPS 48-h forecast has tightly coupled the TC with the first short-wave trough, which has rapidly increased the poleward displacement of the combined circulation. Notice that in both forecasts, the system remains vertically coupled, although only a weak open 500-mb trough is present in the NOGAPS forecast. Thus, it does not appear that vertical wind shear is impacting the track forecasts at 48 h.

By 72 h, the 500-mb NOGAPS analysis (Fig. 3.9d) has represented the Anacelle remnants as a weak open wave above the 72-h forecast position near 41°S, 82°E and below a jet maximum in a strong northwesterly flow. In the ECMWF 72-h forecast (Fig. 3.9l), the position of Anacelle appears to be connected with a jet maximum to the northeast, whereas Anacelle is actually moving southeastward in conjunction with a jet maximum to the east and southeast (Fig.

3.9d). By contrast, the NOGAPS 72-h forecast (Fig. 3.9h) still has a nearly closed circulation adjacent to a much too-strong northwesterly flow. That is, the NOGAPS model has predicted an Excessive BCI as in the conceptual model (Fig. 3.8). Although the NOGAPS model has correctly forecast the poleward acceleration of the TC remnants, the too-strong cyclogenesis has also led to a westward displacement relative to the actual position.

These differences between the NOGAPS and ECMWF 500-mb forecasts have corresponding sea-level pressure forecast differences (Fig. 3.10a-l) that agree quite well with the E-BCI and I-BCI conceptual models in Fig. 3.8. In the ECMWF 24-h forecast (Fig. 3.10j), a small lobe of low pressure extends southeastward from the Anacelle circulation, but does not appear in the corresponding NOGAPS forecast (Fig. 3.10f) or verifying analysis (Fig. 3.10b). This sea-level pressure lobe in a model forecast is a possible symptom of an insufficient interaction of the TC with the low-level cyclogenesis associated with the upper-level midlatitude trough in Fig. 3.9j. However, the relatively good agreement of the ECMWF 24-h forecast position with the verifying position (Fig. 3.9a) indicates that the I-BCI error mechanism has not yet significantly degraded the performance of ECMWF model.

A lobe of low pressure extending southeastward from Anacelle is an indicator that the actual BCI process has begun at 48 h (Fig. 3.10c), but is much more extensive in the ECMWF 48-h forecast (Fig. 3.10k). The appearance of a well-defined lobe in the ECMWF 48-h forecast indicates that significant I-BCI is degrading the model. By contrast, the larger size and lower central pressure of the TC, as well as the more rapid poleward displacement, in the NOGAPS 48-h forecast (Fig. 3.10g) compared to the verifying analysis (Fig. 3.10c) is consistent with an E-BCI error mechanism in that model. These manifestations of I-BCI and E-BCI in ECMWF and NOGAPS, respectively, continue during the next 24 h, which results in an increased equatorward (poleward) bias in the ECMWF (NOGAPS) 72-h forecast position (Fig. 3.10a).
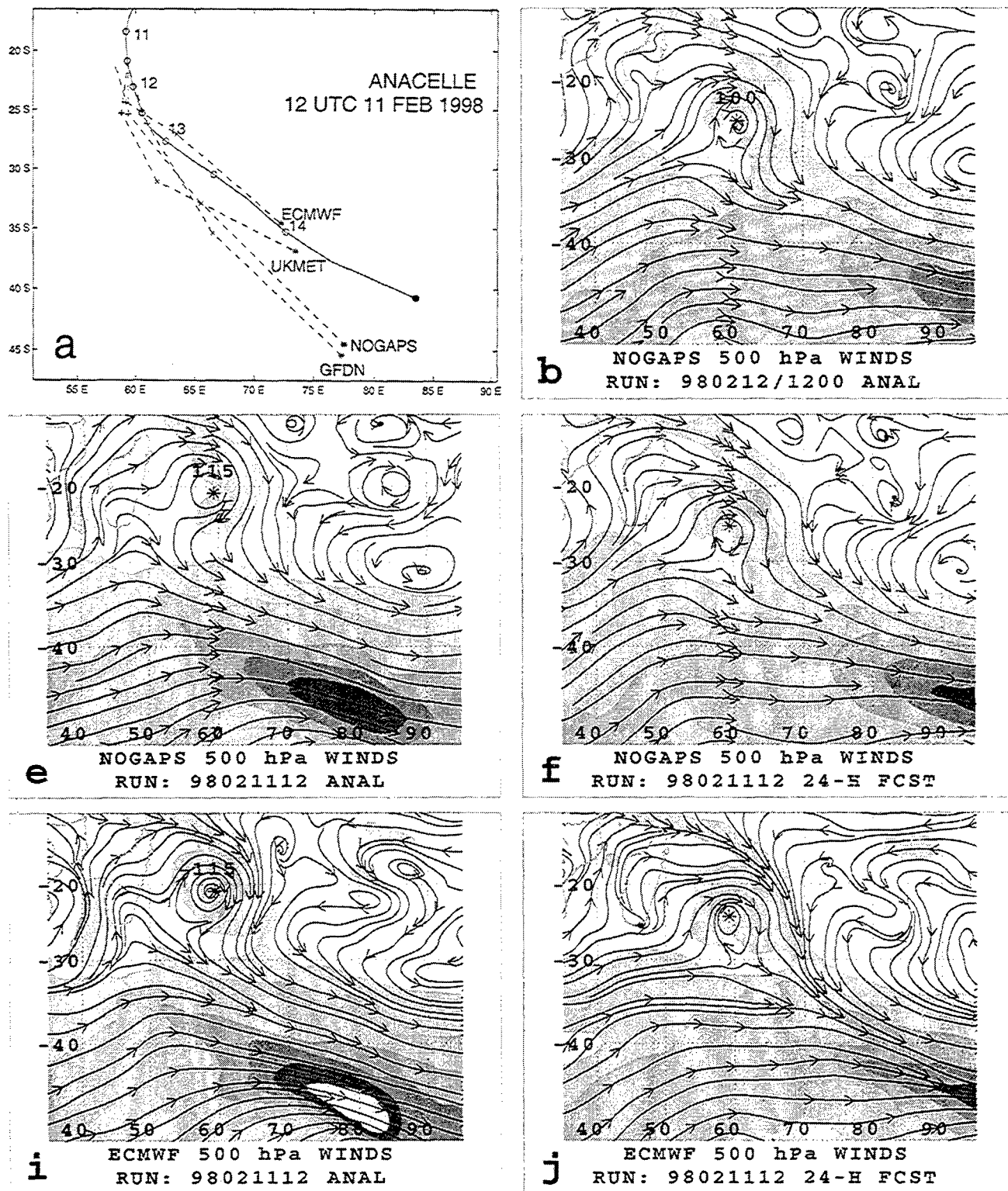
Fig. 3.9 Tracks (panel a) and 500-mb streamline/isotach analyses (panels b-d) and NOGAPS (panels f-h) and ECMWF (panels j-l) forecasts as in Fig. 3.2, except for TC Anacelle beginning at 1200 UTC 11 February 1998.
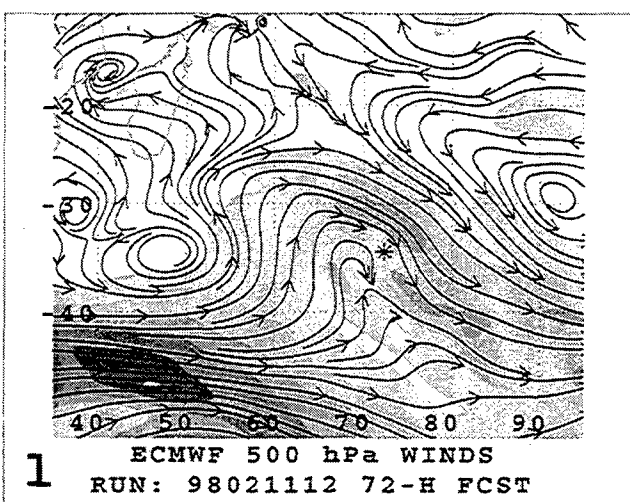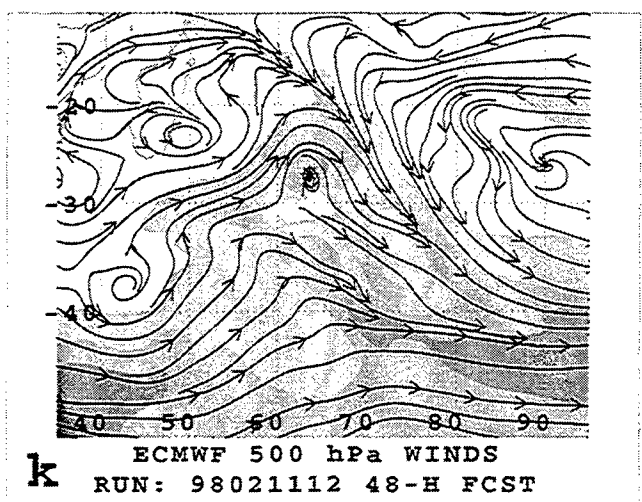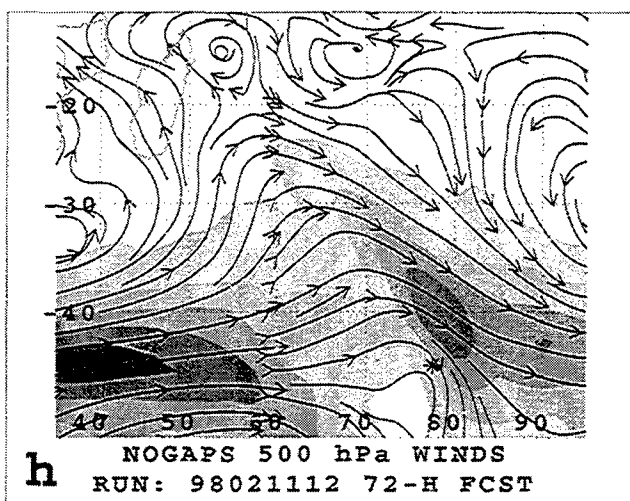
c   NOGAPS 500 hPa WINDS
     RUN: 980213/1200 ANAL

d   NOGAPS 500 hPa WINDS
     RUN: 980214/1200 ANAL

g   NOGAPS 500 hPa WINDS
     RUN: 98021112 48-H FCST

h   NOGAPS 500 hPa WINDS
     RUN: 98021112 72-H FCST

k   ECMWF 500 hPa WINDS
     RUN: 98021112 48-H FCST

l   ECMWF 500 hPa WINDS
     RUN: 98021112 72-H FCST
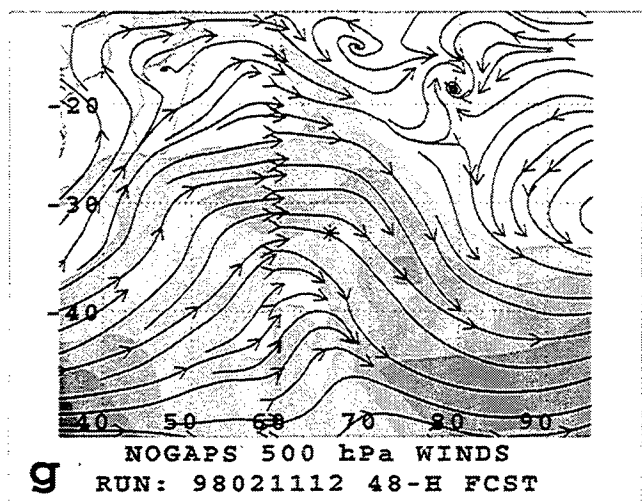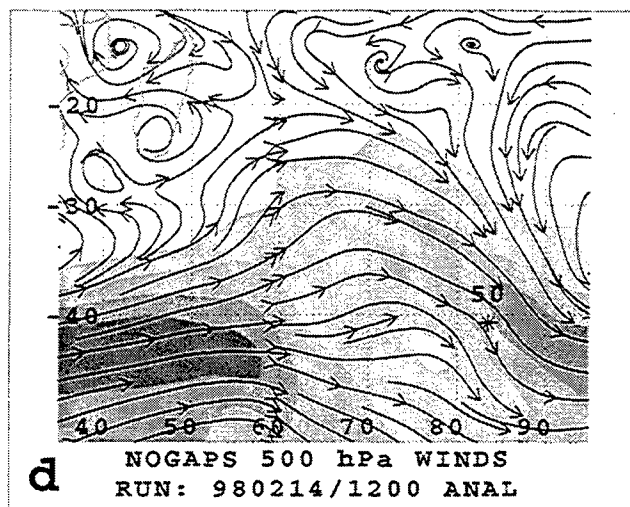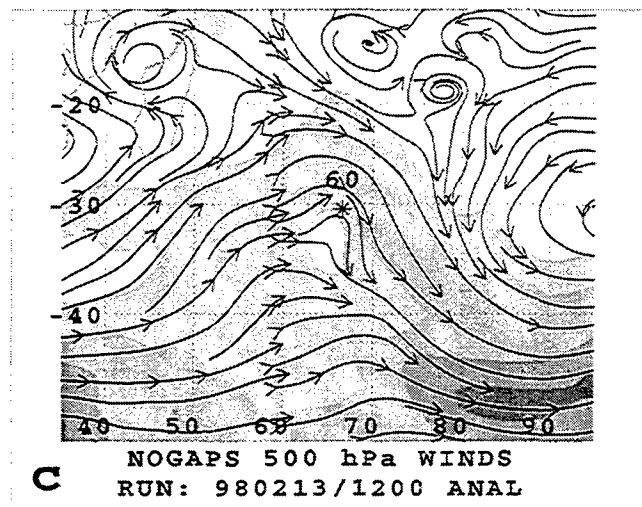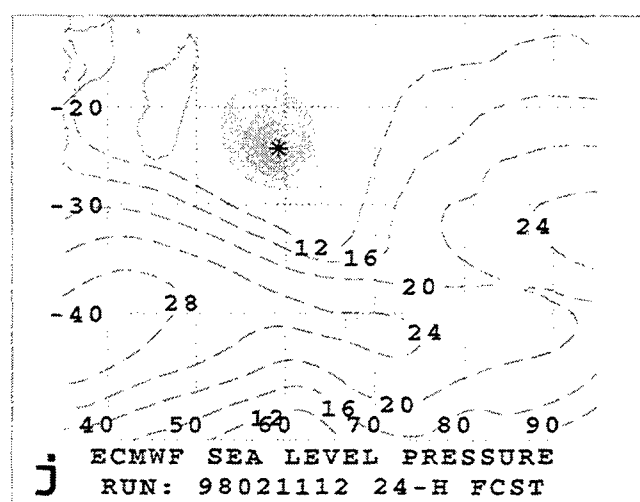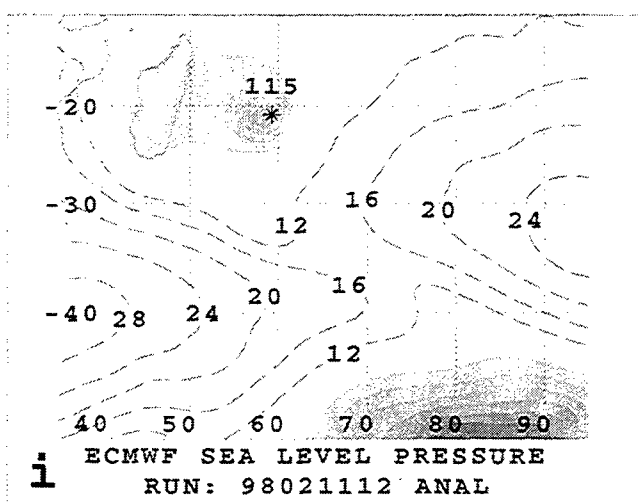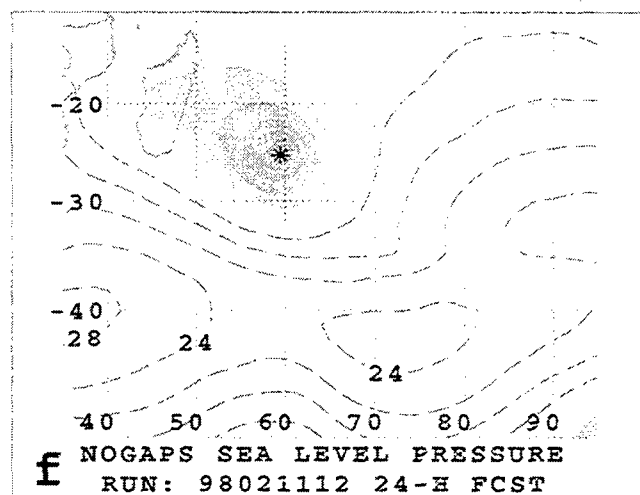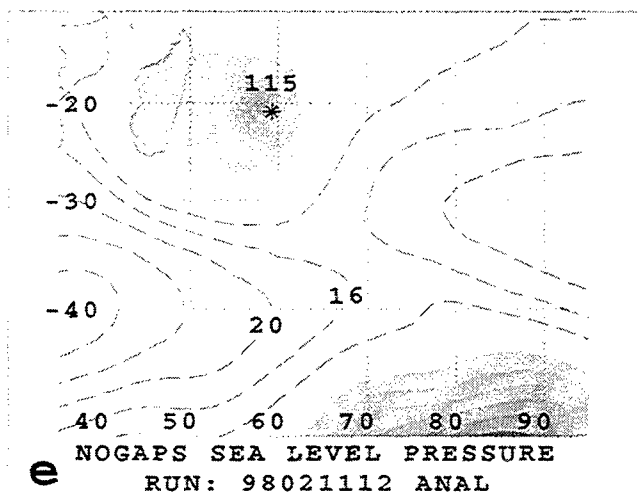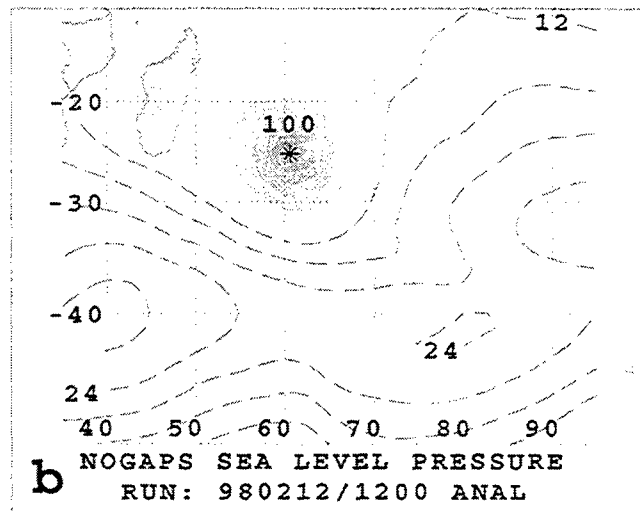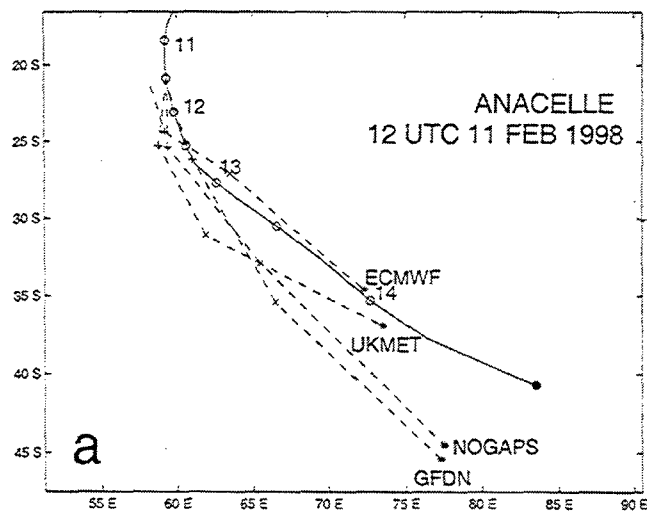
Fig. 3.9 (continued)

Fig. 3.10 Tracks (panel a) and sea-level pressure analyses (panels b-d) and NOGAPS (panels f-h) and ECMWF (panels j-l) forecasts corresponding to Fig. 3.9 for TC Anacelle.

c NOGAPS SEA LEVEL PRESSURE
   RUN: 980213/1200 ANAL

d NOGAPS SEA LEVEL PRESSURE
   RUN: 980214/1200 ANAL

g NOGAPS SEA LEVEL PRESSURE
   RUN: 98021112 48-H FCST

h NOGAPS SEA LEVEL PRESSURE
   RUN: 98021112 72-H FCST

k ECMWF SEA LEVEL PRESSURE
   RUN: 98021112 48-H FCST

l ECMWF SEA LEVEL PRESSURE
   RUN: 98021112 72-H FCST

Fig. 3.10 (continued)

37
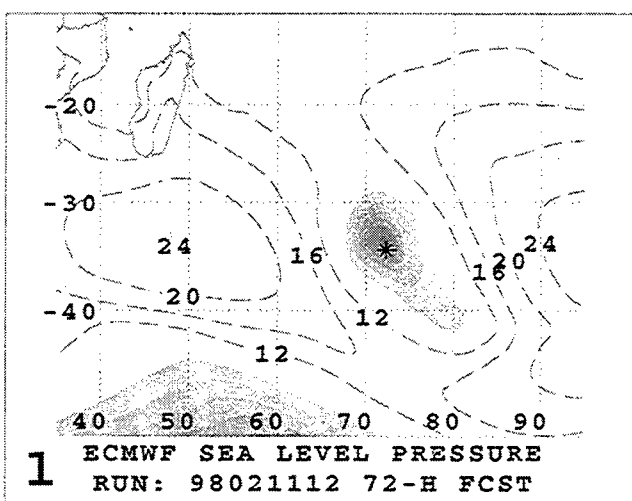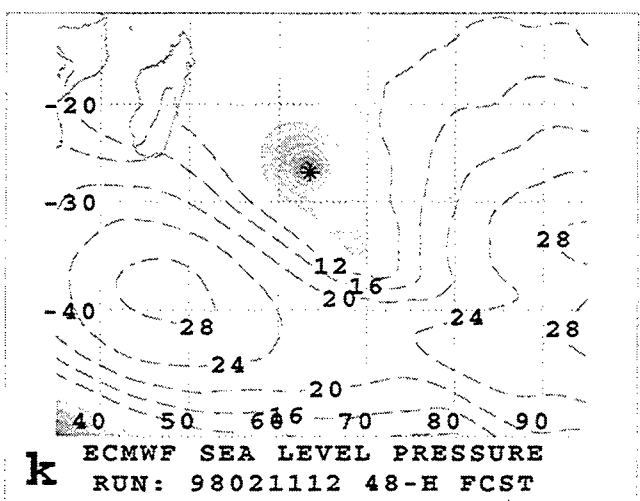
4. Primarily tropical region error sources

As indicated in Table 2.2, the only frequently (> 10% of all large track errors) occurring tropical region error source for this Southern Hemisphere sample was Direct Cyclone Interaction (DCI), which was the most frequently occurring error source in the western North Pacific (Table 2.1). Another frequent western North Pacific tropical error source is the Ridge Modification by the TC (RMT), which did contribute about 9% of the GFDN track errors (Table 2.2). The E-RMT error is associated with either too large a TC or a Rossby wave train generated by a large cyclone (tropical or extratropical) to the southwest of a Southern Hemisphere TC. Since an error in the Southern Hemisphere initial TC specification for GFDN has been discovered (and corrected in May 2000) at the Fleet Numerical Meteorology and Oceanography Center, this E-RMT error source will not be discussed here. Thus, the only tropical error source to be described is the DCI.

a. Description of Direct Cyclone Interaction (DCI) error

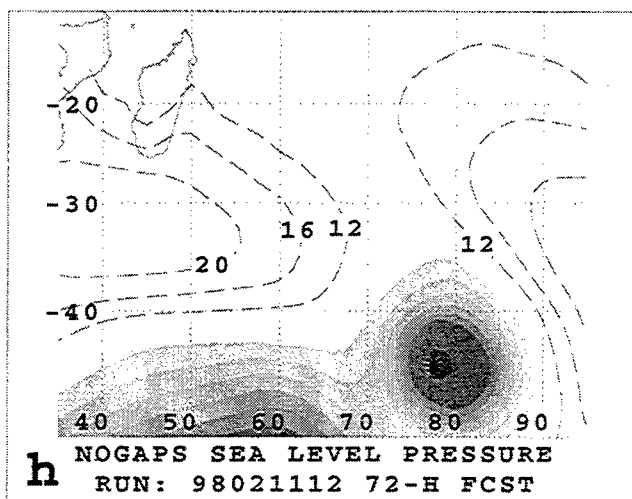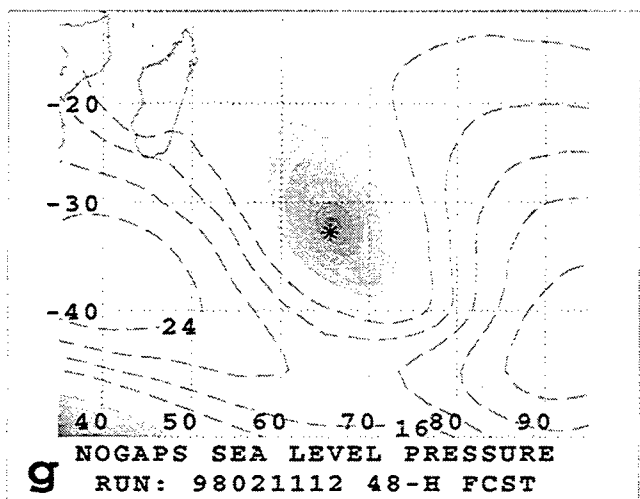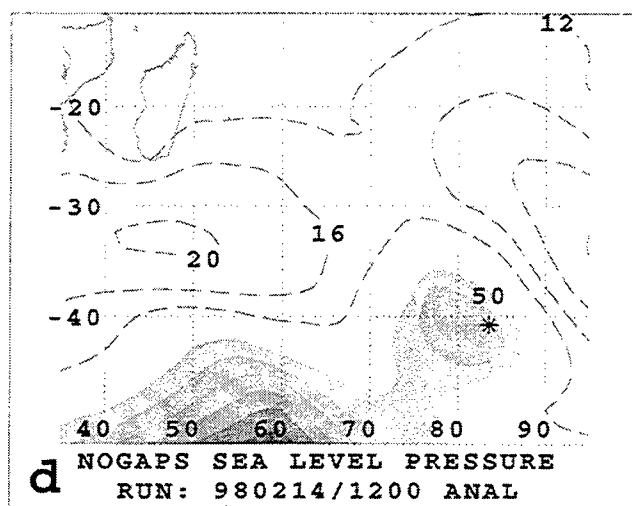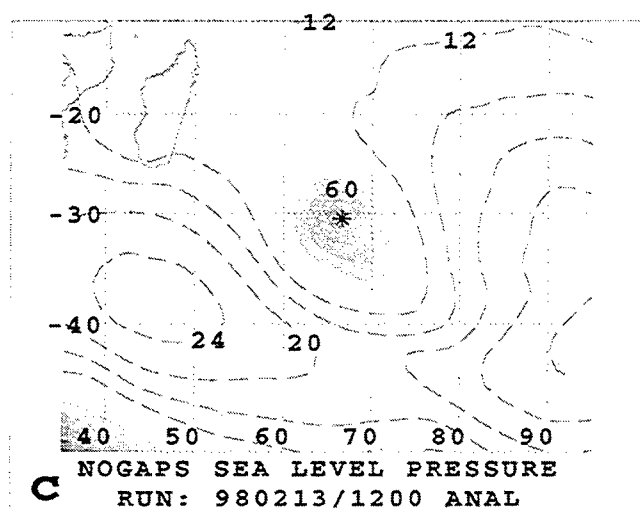All three of the modes of binary cyclone interaction (i.e., direct, semi-direct, and indirect) defined by Carr et al. (1997) were discovered to be causes for the NOGAPS, GFDN, UKMO, or ECMWF track errors (Table 2.2). Excessive DCI was responsible for about 27%, 14%, 18%, and 11%, respectively of all highly erroneous track forecasts in the Southern Hemisphere. Nearly all of the Semi-direct Cyclone Interaction (SCI) errors are for the eastern or western TCs rather than SCI with north-south oriented TCs. Since the SCIE and SCIW errors were infrequent in this sample, the reader is referred to Carr and Elsberry (1999) for a description and conceptual model based on the western North Pacific TCs. The SCI on a poleward or an equatorward TC described by Bannister et al. (1998) occurs rarely, and only the SCIQ led to a track error with the GFDN model only (Table 2.2). An *Insufficient* SCIQ may arise when the equatorward TC is the target of the initial TC specification in the GFDN model, so that the poleward TC may not have been adequately represented. Finally, so few cases of ICI errors occurred that this error source is not discussed further. A description/conceptual model of the ICI error mechanism for the western North Pacific is given in Carr and Elsberry (1999).

An *Excessive* DCI (E-DCI) error occurs when the TC circulation is forecast to directly interact with an adjacent cyclonic circulation such that the predicted interaction is either false or is significantly more vigorous than in reality (Fig. 4.1). The concept of DCI is analogous to the Direct TC Interaction described by Carr et al. (1997), except that the adjacent cyclone in the analysis or forecast is not necessarily a TC. If real, the other cyclone may be: (i) a named TC or a remnant circulation; (ii) a tropical disturbance that does not develop into a named TC; or (iii) an upper-tropospheric circulation of midlatitude origin. In general, the E-DCI errors tend to occur when the TC is moving westward in the vicinity of the monsoon trough, or recently has turned poleward, but is still in proximity to the tropical easterlies. The E-DCI errors often occur when the TC is a moderate tropical storm (< 50 kt; 25 m s^{-1}) or depression, because a dynamical model misrepresentation of a nearby cyclone would be expected to have a greater impact on the model-predicted track of a weak TC.
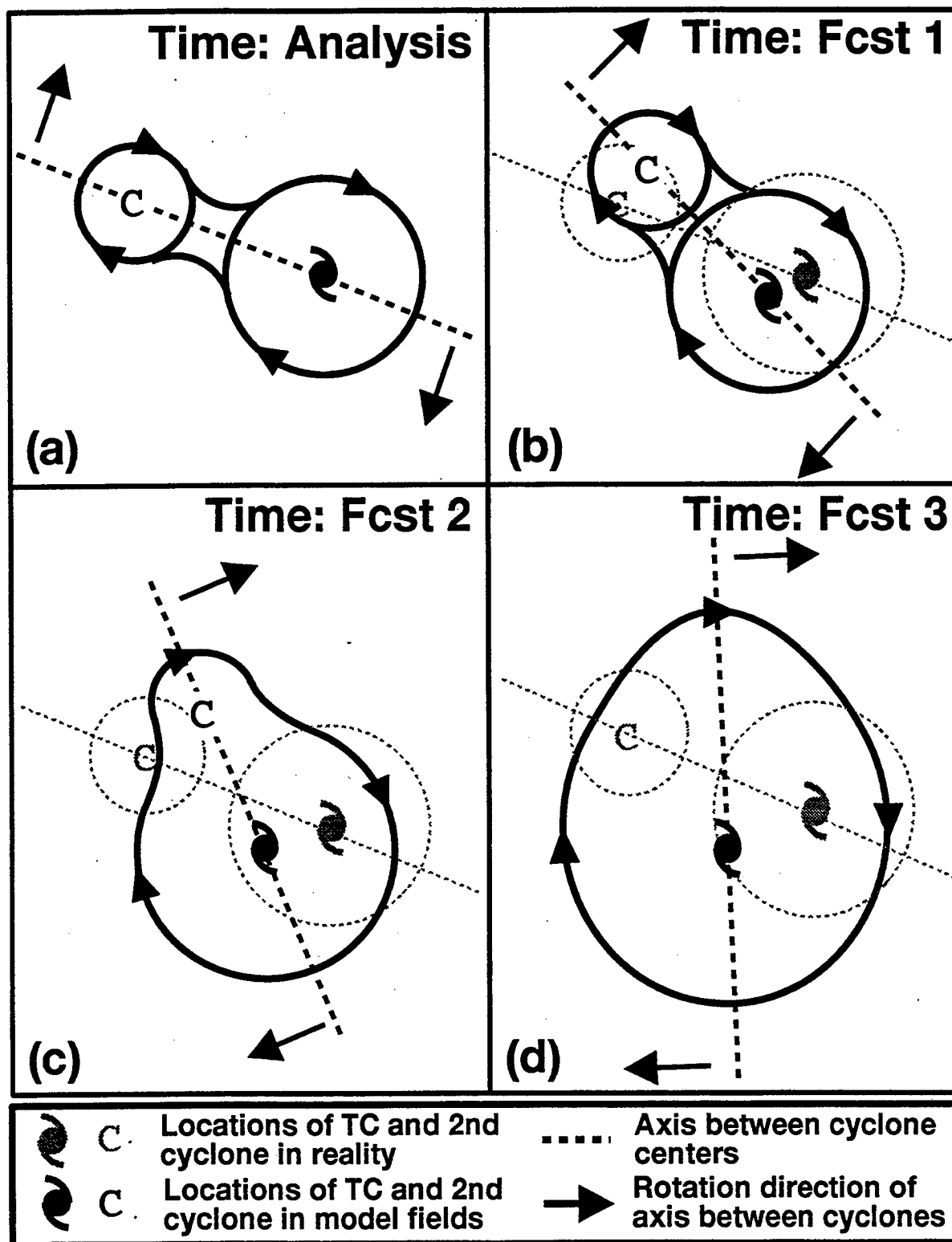
Fig. 4.1 Conceptual model of Excessive-Direct Cyclone Interaction (E-DCI) in which a TC circulation interacts with another cyclone (C) to cause a clockwise (Southern Hemisphere) rotation of the axis between the cyclone centers (heavy dashed line) and a possible merger of the two cyclones in which the combined circulation becomes larger with time (panels c and d). The TC may also be the smaller of the two cyclones, or the model may be applied to two TCs of similar sizes in which the tracks of both TCs will be affected.

39

Notice that the conceptual model of E-DCI (Fig. 4.1) involves an apparent cyclonic rotation (clockwise in the Southern Hemisphere) of the two cyclones and a possible merger into one circulation that is usually larger in size than the analyzed TC. The TC in Fig. 4.1 is depicted as the larger, and thus more dominant, circulation into which the second smaller cyclone merges. In this case, the TC track forecast by the model may be only moderately affected by the interaction, since such an interaction depends on the strength of the other cyclone. It is also possible that the second cyclone will be analyzed and forecast in the model to be the dominant circulation into which the TC tends to merge. In this case, the TC track forecast by the model will often exhibit a definite cyclonic loop, and the forecast track may be prematurely terminated owing to excessive weakening of the model TC as it merges with the overly strong adjacent cyclone.

Reasons for E-DCI with another real cyclonic circulation include: (i) too large a horizontal extent and associated outer wind strength of the TC and/or the other cyclone in the initial analysis, or during the forecast (Fig. 4.1); (ii) mis-location of the TC and/or the other cyclone in the initial analysis, or during the forecast such that the separation of the two cyclones is smaller than in reality; and (iii) overly deep penetration of an upper-level midlatitude circulation into the lower troposphere where it can affect the steering of the TC. It is also possible for numerical models to forecast E-DCI between the TC and a fictitious cyclone. This scenario was found to be relatively rare in this Southern Hemisphere sample.

Another situation that has been occasionally observed in the NOGAPS model, but not in the GFDN model, is a self-interaction caused by a significant difference between the TC location in the first-guess field and the synthetic TC cyclone inserted during the data assimilation cycle. As a result, the NOGAPS initial analysis contains two non-collocated representations of the same TC that will then tend to rotate around each other during the early stages of the model integration. This phenomenon may occur when: (i) the warning position, about which the synthetic observations are centered, is significantly offset from the initial position in the 12-h NOGAPS forecast that serves as the first-guess for the analysis; or (ii) a significant relocation of the analysis position or short-term forecast occurs between two successive synoptic times. These situations are less likely to occur in the GFDN model because the TC vortex is effectively removed by filtering the global model analysis before a model-compatible vortex is inserted at the warning position.

b.   *Case study of Excessive-Direct Cyclone Interaction (E-DCI)*

The case of Cathy on 0000 UTC 25 December 1998 involves an actual case of DCI between Cathy and a broad, weak tropical depression (TD). Satellite imagery (not shown) documents the existence of the weak TD southwest of Sumatra, and Cathy is to the south-southeast of the TD. One of the characteristic tracks in a DCI with the cyclone to the northeast or east is an equatorward deflection of the TC. As illustrated in Fig. 4.2a, the Cathy track does turn toward the west-northwest beginning on 27 December.

Disparities between UKMO and NOGAPS initial analyses are illustrated in Figs. 4.2e and i, respectively. The monsoon trough in the UKMO analysis is along 6°-7°S between 70°E and 95°E, with a broad, closed cyclone to the northwest of Cathy. The NOGAPS analysis has a

buffer-type trough on, or even north of, the Equator, with only a weak trough extending northwestward from Cathy. The subtropical anticyclone cell poleward of TS Cathy (just 35 kt at the initial time) is also more intense in the UKMO analysis than an open ridge in the NOGAPS analysis. Such initial analysis differences over the central South Indian Ocean can occur in this data-sparse region. The UKMO initial analysis 24 h later (Fig. 4.2b) clearly separates a well-defined 500-mb cyclonic circulation that is Cathy from a monsoon trough cell near 8°S, 90°E. Given the westward translation at this time (26 December) in Fig. 4.2a, the isotach maximum to the southeast (versus to the south) in the UKMO analysis indicates some continuing problems in the analysis.

Already by 24 h, dramatic changes occur in the UKMO (Fig. 4.2f) and NOGAPS (Fig. 4.2j) forecasts. The TC weakens as it translates westward in the UKMO forecast as a wave rotating cyclonically around the monsoon trough circulation. Thus, the TC has rotated cyclonically about 45° from a southeastward location 24 h ago to almost directly south of the monsoon trough cell. A similar cyclonic rotation is predicted in the NOGAPS 24-h forecast, with a translation toward the northwest of an open wave that represents Cathy. This immediate equatorward deflection of the NOGAPS track from a persistence track toward the west (Fig. 4.2a) would certainly be a clue to the forecaster about a likely error.

At 48 h, the UKMO analysis (Fig. 4.2c) indicates a relative cyclonic rotation between the westward-moving TC and the eastward displacement of the monsoon trough circulation. The subtropical anticyclone cell has been analyzed poleward of the TC more like the initial analysis (Fig. 4.2e) than in the 24-h analysis (Fig. 4.2b). Consequently, the isotach maximum to the south of TC Cathy is again consistent with the westward motion.

By 48 h, the TC and monsoon trough circulation appear to be merging in the UKMO forecast (Fig. 4.2g). Notice the western lobe that represents the TC in the merged circulation represents a nearly 90° cyclonic rotation over the past 24 h (compare with Fig. 4.2f where the lobe is to the south). Furthermore, this represents a northwestward displacement between 24 h and 48 h in the UKMO forecast track (Fig. 4.2a). The two circulations have also merged into a broad, poorly defined feature in the NOGAPS 48-h forecast (Fig. 4.2k).

In the verifying analysis at 72 h (Fig. 4.2d), the weakened TC is separate from the monsoon trough. However, the merged TC-monsoon cell circulation in the UKMO 72-h forecast (Fig. 4.2h) is a large cell that is translating to the northwest. The 1000-mb wind tracker in the NOGAPS places the 72-h position near 10°S, 87°E. Only a weak reflection of this circulation is indicated in the 500-mb circulation by the oblong streamlines to the east-southeast of the track forecast position (Fig. 4.2l).

The cyclonic rotation of TC Cathy and the monsoon trough cell is revealed well in their associated 850-mb vorticity maxima (Fig. 4.3). The monsoon trough maximum is initially (Fig. 4.3a) near 7°S, 93°E at 0000 UTC 27 December 1998 (Fig. 4.3d). The cyclonic vorticity maximum associated with Cathy moves westward from near 16°S, 97°E at the initial time to 16°S, 93°E by 48 h. Thus, a cyclonic rotation of the axis connecting these two vorticity maxima has in nature as in the DCI mechanism (Carr *et al.* 1997). By 24 h in the UKMO forecast (Fig. 4.3c), the two vorticity maxima have rotated more rapidly and the separation distance has

a CATHY 00 UTC 25 DEC 1998

b UKMET 500 hPa WINDS RUN: 981226/0000 ANAL

e UKMET 500 hPa WINDS RUN: 98122500 ANAL

f UKMET 500 hPa WINDS RUN: 98122500 24-H FCST

i NOGAPS 500 hPa WINDS RUN: 98122500 ANAL

j NOGAPS 500 hPa WINDS RUN: 98122500 24-H FCST
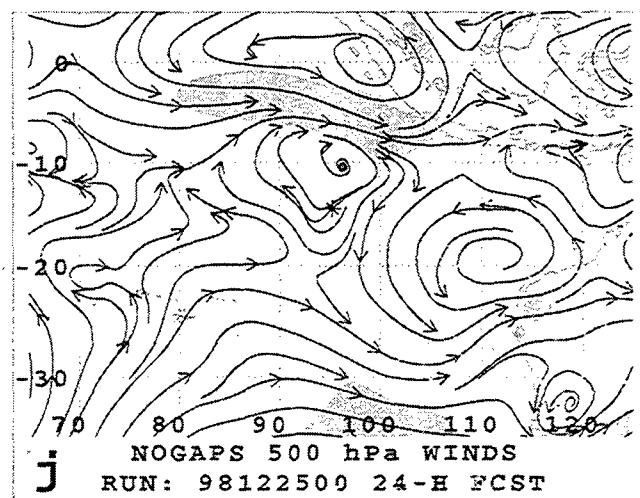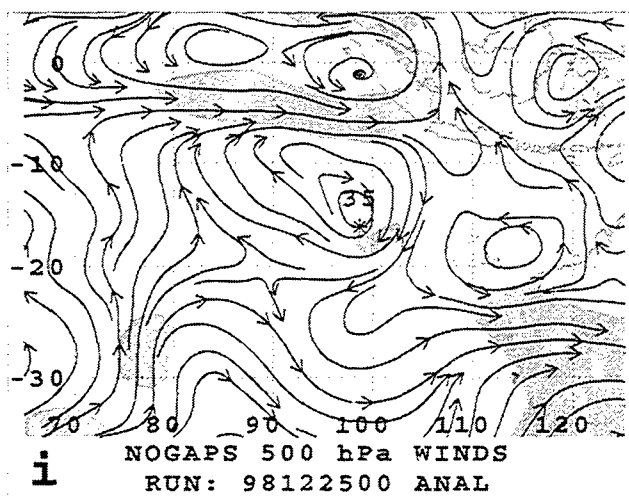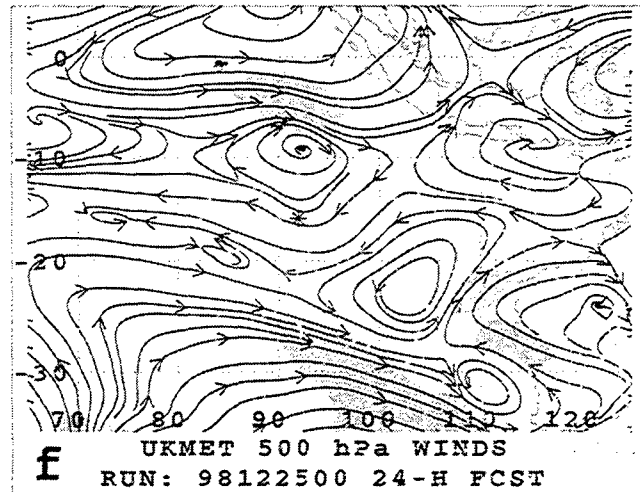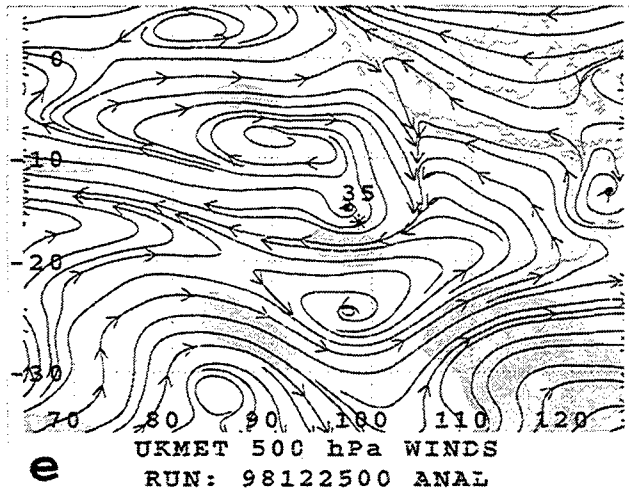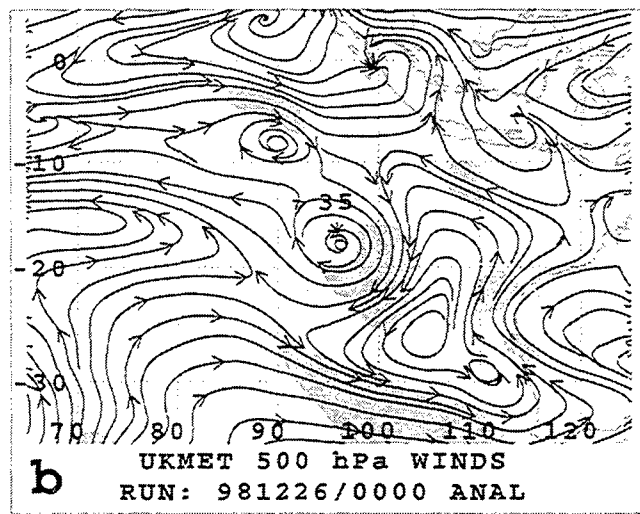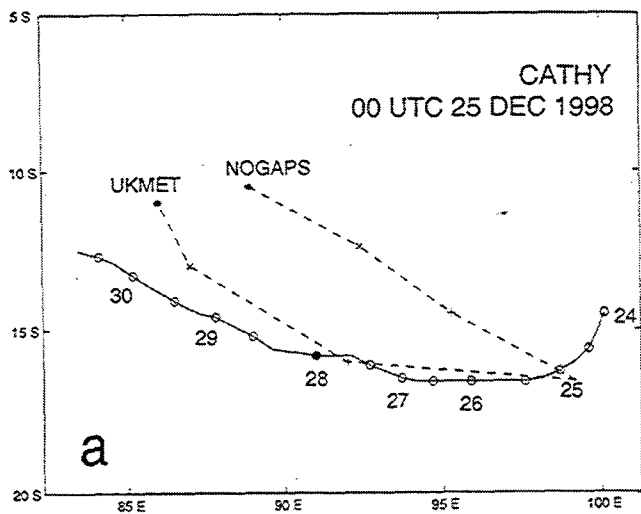
Fig. 4.2 Tracks (panel a) and 500-mb streamline/isotach analyses (panels b-d) and UKMO (panels f-h) and NOGAPS (panels j-l) forecasts as in Fig. 3.2, except for TC Cathy beginning at 0000 UTC 25 December 1998.

c   UKMET 500 hPa WINDS
     RUN: 981227/0000 ANAL

d   UKMET 500 hPa WINDS
     RUN: 981228/0000 ANAL

g   UKMET 500 hPa WINDS
     RUN: 98122500 48-H FCST

h   UKMET 500 hPa WINDS
     RUN: 98122500 72-H FCST

k   NOGAPS 500 hPa WINDS
     RUN: 98122500 48-H FCST

l   NOGAPS 500 hPa WINDS
     RUN: 98122500 72-H FCST

Fig. 4.2 (continued)

43
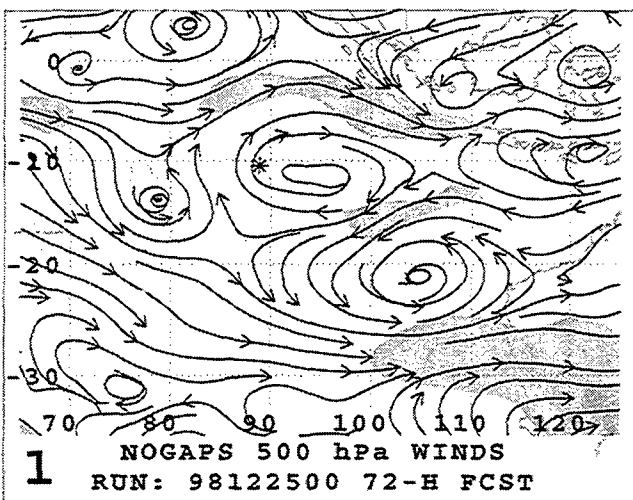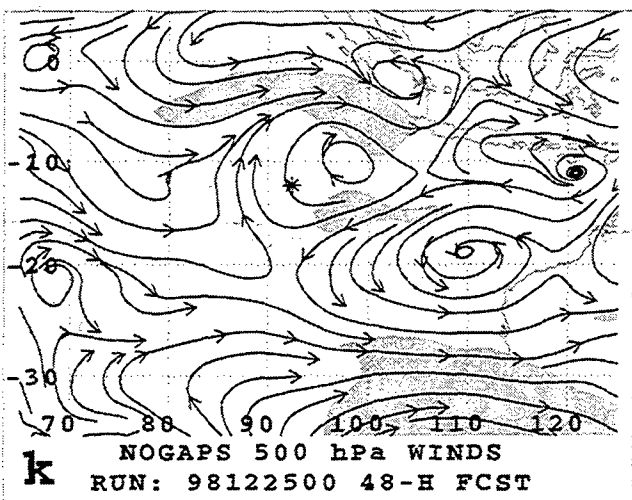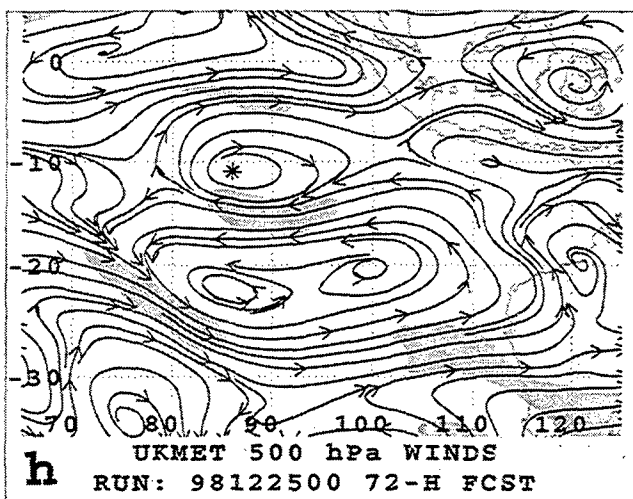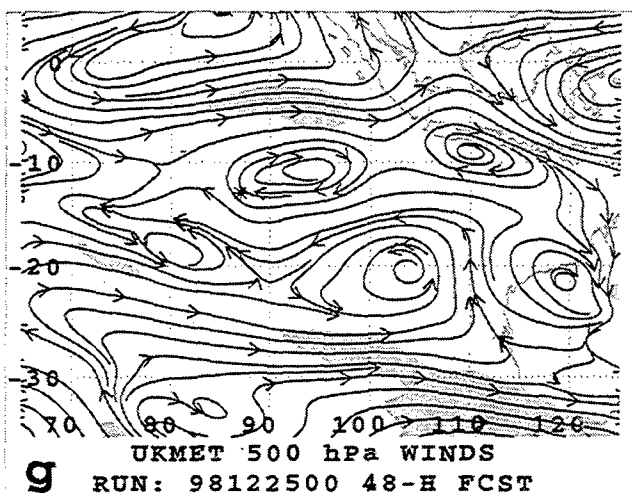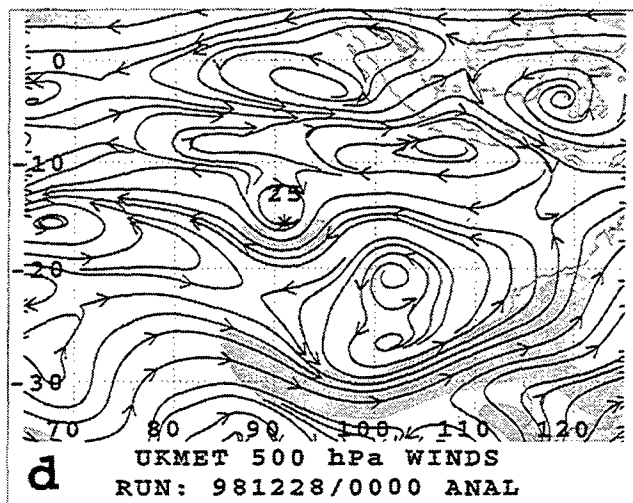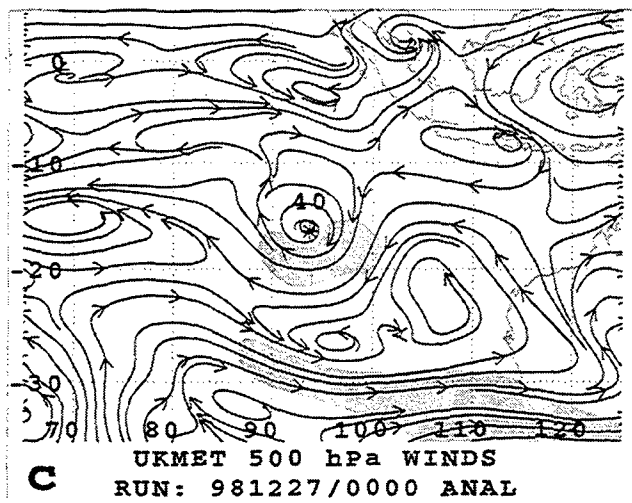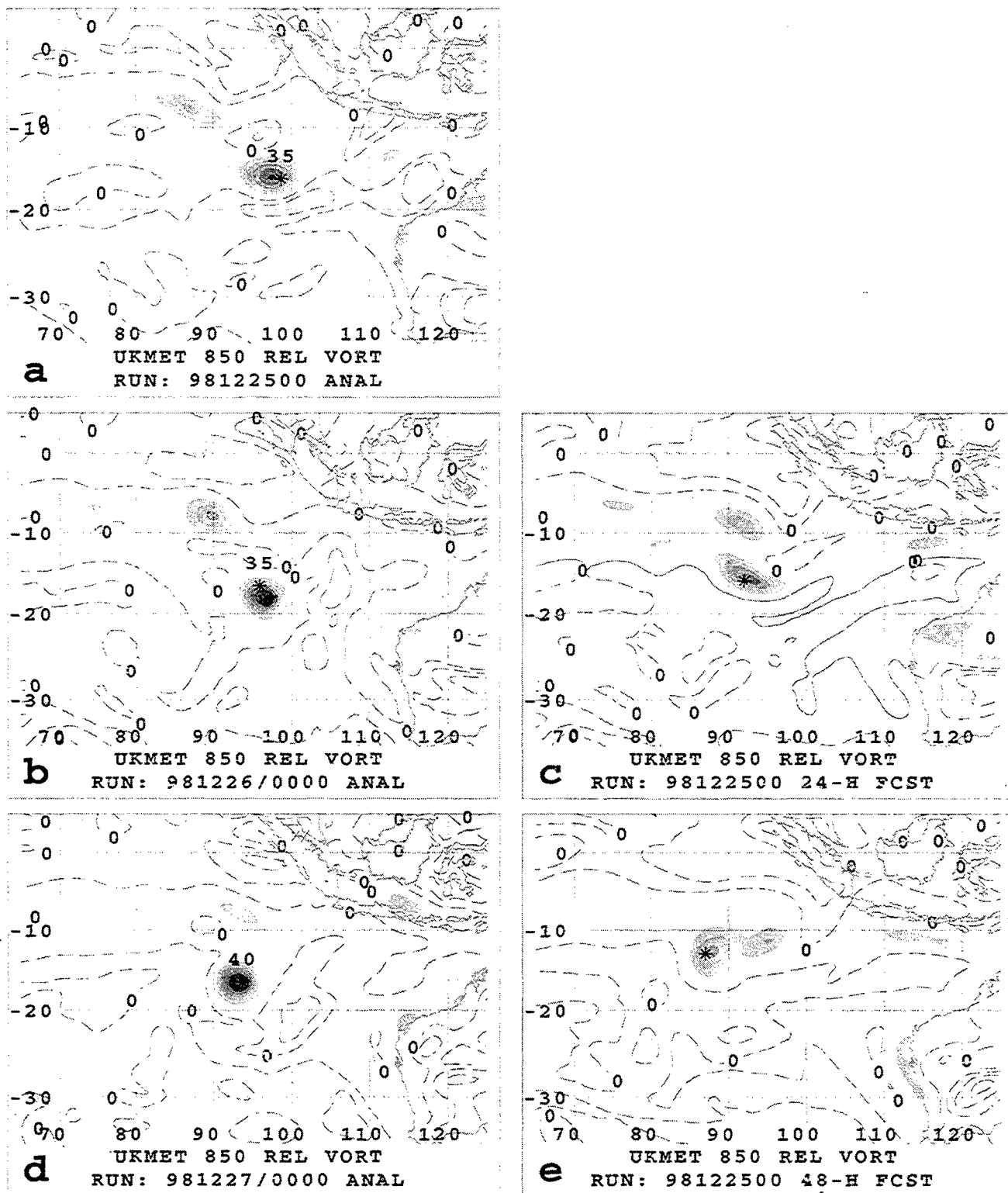
Fig. 4.3 Relative vorticity (cyclonic shaded beginning at - 2 $(10^{-5})s^{-1}$ with contour interval of 2 $(10^{-5})s^{-1}$ from the UKMO 850-mb analyses at 0000 UTC on 25, 26, and 27 December 1998 (panels a, b, and d, respectively) and corresponding UKMO forecasts at (c) 24 h and (e) 48 h. Whereas the monsoon trough vorticity maximum (top) and TC vorticity maximum (lower) rotate in the analyses, the rotation is more rapid in the forecasts.

decreased, which indicates Excessive DCI compared to the actual DCI. The elongation of each vorticity maximum in a cyclonic circulation sense is another clue that DCI is predicted in the UKMO model. By 48 h (Fig. 4.3e), the excessive cyclonic rotation and tendency to merge the two circulations in the model is quite evident.

In real-time, the forecaster is confronted with a dilemma. Since the monsoon trough cell and the TC are within the separation distance for DCI (Carr *et al.* 1997), it is likely that DCI will occur. However, will the DCI be as vigorous as indicated by the UKMO and NOGAPS forecasts? The evidence in both the western North Pacific and this Southern Hemisphere study (Table 2.1) would indicate that E-DCI should be expected, especially as I-DCI is rarely observed in the global models. Thus, the best odds for this forecast would be to downplay the cyclonic rotation and extreme equatorward displacements in the UKMO and NOGAPS tracks (Fig. 4.2a).

5. Concluding remarks

This research extends to the Southern Hemisphere the procedures used by Carr and Elsberry (1999, 2000a, b) to search for the sources of large (> 300 n mi) 72-h errors in the dynamical tropical cyclone (TC) track predictions. Except for two cases related to Equatorial Westerly wind Bursts, the same large-error conceptual models that Carr and Elsberry developed for the western North Pacific also apply in the Southern Hemisphere. As summarized in Table 2.1, the distributions of frequently occurring error sources differ between the two TC basins. Those error sources related to Midlatitude System Evolutions (MSE), Response to Vertical wind Shear (RVS), and Baroclinic Cyclone Interaction (BCI) are more frequent in the Southern Hemisphere than Carr and Elsberry found in the western North Pacific.

This predominance for midlatitude-related errors (versus the more frequent tropical-related errors in the Carr and Elsberry study) is not really surprising in view of the importance of the High-amplitude (H) synoptic pattern in affecting Southern Hemisphere TC motion (Bannister et al. 1997, Reader et al. 1999). Each of the Carr and Elsberry large-error conceptual models involves the dynamical model incorrectly predicting a known physical cause of TC motion. In the H pattern, the model may incorrectly handle the deeply penetrating trough-ridge system, the TC circulation, or the adjacent tropical circulations. Thus, contributions to the dynamical model track errors in the H pattern may come from multiple sources.

The one frequently occurring tropical-related error source in the Southern Hemisphere was the Excessive-Direct Cyclone Interaction, which was the overall most frequent error source for the western North Pacific sample of Carr and Elsberry. Similar reasons for the dynamical models having a E-DCI error apply in both regions, it is just that the frequency of tropical circulations near enough to the TC to contribute to DCI is smaller in the Southern Hemisphere.

This is a retrospective study in which it is known that the dynamical model track error exceeds 300 n mi, and the objective is to isolate the error source. As noted in Chap. 3, more than one midlatitude error source may be contributing, and the goal here was to identify the most important source. It is helpful to know what physical mechanisms (environmental or TC-related) are causing the TC to move with a particular direction/speed, and any transitional mechanisms that are present. Given this information, the possible ways in which the dynamical model may be mishandling the situation are somewhat limited, which is useful information to the forecaster.

The real goal of this research is to help the forecaster identify likely erroneous tracks in real-time. The frequently occurring error sources identified in this research are a part of the dynamical Model Traits knowledge base in the Systematic Approach (Fig. 1.2). Preliminary experience in the western North Pacific suggests it is possible to use an expert system to guide the forecaster in identifying dynamical model tracks that should be discarded (Carr et al. 2000). Future research will determine if these conceptual models and expert system will also be successful in the Southern Hemisphere.

A Systematic Approach Meteorological knowledge base for the Southern Hemisphere has been developed by Bannister *et al.* (1997, 1998) and Reader *et al.* (1999). Key components for this study are the transitional mechanisms (in the bottom half of diagram) that lead to environment structure changes. If the dynamical model incorrectly predicts (either excessively or insufficiently) these transitional mechanisms, it is likely that a 72-h track error > 300 n mi will result.

Meteorological Knowledge Base for the Southern Hemisphere

ENVIRONMENT STRUCTURE

PATTERN

Standard (S)   Poleward (P)
High-amplitude (H)   Midlatitude (M)

REGION
Equatorial Westerlies (EW)
Tropical Easterlies (TE)
Poleward Flow (PF)
Equatorward Flow (EF)
Ridge Poleward (RP)
Ridge Equatorward (RE)
Trough Poleward (TP)
Midlatitude Westerlies (MW)
Midlatitude Easterlies (ME)

TC STRUCTURE

INTENSITY

Exposed Low-level (XL)
Tropical Depression (TD)
Tropical Storm (TS)
Typhoon (TY)
Super Typhoon (STY)

SIZE

Midget (M)   Average (A)
Small (S)   Large (L)

ENVIRONMENT EFFECTS

Advection by Environment (ADV)
Tropical Environment Evolutions:
  Equatorial Westerly Wind Burst (EWB)
Midlatitude System Evolutions (MSE):
  Cyclogenesis (MCG)
  Cyclolysis (MCL)
  Anticyclogenesis (MAG)
  Anticyclolysis (MAL)

TC-ENVIRONMENT TRANSFORMATIONS

Beta Effect-Related:
  Beta-Effect Propagation (BEP)
  Ridge Modification by TC (RMT)
  Reverse Trough Formation (RTF)
Cyclone Interactions:
  Direct Interaction (DCI)
  Semidirect Interaction (SCI)
  Indirect Interaction (ICI)
Midlatitude-Related:
  Response to Vertical Shear (RVS)
  Baroclinic Cyclone Interaction (BCI)

TRANSITIONAL MECHANISMS

The environment structures (synoptic patterns and regions) included in the Meteorological knowledge base on the previous page are depicted in these schematics of the streamflows and TC track segments. See Reader *et al.* (1999) for explanations.
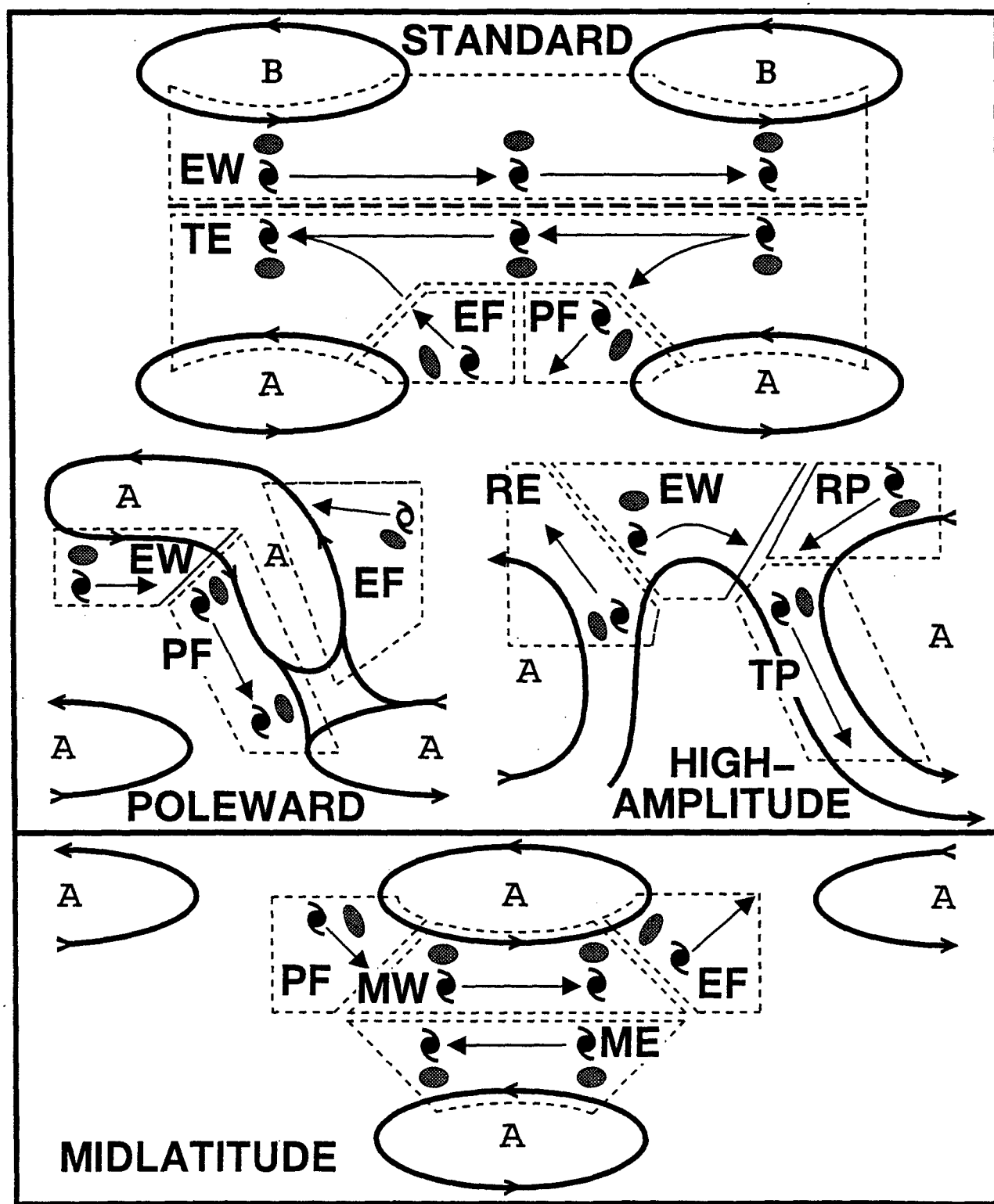
REFERENCES

Bannister, A. J., M. A. Boothe, L. E. Carr, III, and R. L. Elsberry, 1997: Southern Hemisphere application of the Systematic Approach to tropical cyclone track forecasting. Part I. Environmental structure characteristics. Tech. Rep. NPS-MR-98-001, Naval Postgraduate School, Monterey, CA 93943-5114, 96 pp.

Bannister, A. J., M. A. Boothe, L. E. Carr, III, and R. L. Elsberry, 1998: Southern Hemisphere application of the Systematic Approach to tropical cyclone track forecasting. Part II. Climatology and refinement of Meteorological knowledge base. Tech. Rep. NPS-MR-98-004, Naval Postgraduate School, Monterey, CA 93943-5114, 69 pp.

Brown, D., M. A. Boothe, L. E. Carr, III, and R. L. Elsberry, 2000: Evaluation of dynamical track predictions for tropical cyclones in the Atlantic during 1995-98. Preprints, *24th Conf. Hurr. Trop. Meteor.*, Ft. Lauderdale, FL, Amer. Meteor. Soc., 390-391.

Dunnavan, G. M., L. E. Carr, III, R. L. Elsberry, M. A. Boothe, 2000: Evaluation of dynamical track predictions for tropical cyclones in the western North Pacific: Extensions to other years and dynamical models. Preprints, *24th Conf. Hurr. Trop. Meteor.*, Ft. Lauderdale, FL, Amer. Meteor. Soc., 384-385.

Carr, L. E., III, and R. L. Elsberry, 1994: Systematic and integrated approach to tropical cyclone track forecasting. Part I. Approach overview and description of meteorological basis. Tech. Rep. NPS-MR-94-002, Naval Postgraduate School, Monterey, CA 93943-5114, 273 pp.

Carr, L. E., III, and R. L. Elsberry, 1999: Systematic and integrated approach to tropical cyclone track forecasting. Part III. Traits knowledge base for JTWC track forecast models in the western North Pacific. Tech. Rep. NPS-MR-99-002, Naval Postgraduate School, Monterey, CA 93943-5114, 227 pp.

Carr, L. E., III, and R. L. Elsberry, 2000a: Dynamical tropical cyclone track forecast errors. Part I. Tropical region error sources. *Wea. Forecasting* (in press).

Carr, L. E., III, and R. L. Elsberry, 2000b: Dynamical tropical cyclone track forecast errors. Part II. Midlatitude circulation influences. *Wea. Forecasting* (in press).

Carr, L. E., III, M. A. Boothe, and R. L. Elsberry, 1997a: Observational evidence for alternate modes of track-altering binary tropical cyclone scenarios. *Mon. Wea. Rev.*, **125**, 2094-2111.

Carr, L. E., III, R. L. Elsberry, J. E. Peak, and G. M. Dunnavan, 2000: Development and beta-test of the Systematic Approach Expert System prototype as a tropical cyclone forecasting aid (SAFA). Tech. Rep. NPS-MR-00-002, Naval Postgraduate School, Monterey, CA 93943-5114, 67 pp.

Elsberry, R. L., 1995: Tropical cyclone motion. Chap. 4 in *Global Perspectives on Tropical Cyclones*, (R. L. Elsberry, Ed.), WMO/TD-No. 693, Report No. TCP-38, World Meteorological Organization, Geneva, Switzerland, 106-197.

Elsberry, R. L., and L. E. Carr, III, 2000: Consensus of dynamical tropical cyclone track forecasts--Errors versus spread. *Mon. Wea. Rev.* (in press).

Elsberry, R. L., M. A. Boothe, G. A. Ulses, and P. A. Harr, 1999: Statistical post-processing of NOGAPS tropical cyclone track forecasts. *Mon. Wea. Rev.*, **127**, 1912-1919.

Goerss, J., and R. Jeffries, 1994: Assimilation of synthetic observations into the Navy Operational Global Atmospheric Prediction System. *Wea. Forecasting*, **9**, 557-576.

Heming, J., A. M. Radford, and J. C.-L. Chan, 1995: A new scheme for the initialisation of tropical cyclones in the UK Meteorological Office global model. *Meteor. Apps.*, **2**, 171-184.

Kurihara, Y., M. A. Bender, R. E. Tuleya, and R. J. Ross, 1995: Improvements in the GFDL hurricane prediction system. *Mon. Wea. Rev.*, **123**, 2791-2801.

Reader, G., M. A. Boothe, R. L. Elsberry, and L. E. Carr, III, 1999: Southern Hemisphere application of the Systematic Approach to tropical cyclone track forecasting. Part III: Updated environmental structure characteristics. Tech. Rep. NPS-MR-99-004, Naval Postgraduate School, Monterey, CA 93943-5114, 73 pp.

DISTRIBUTION LIST

Space and Naval Warfare Systems Command   4
PWM 185
4301 Pacific Highway
San Diego, CA 92110-3127

Dr. Carlyle H. Wash, Chairman   1
Department of Meteorology, Code MR/Wx
Naval Postgraduate School
589 Dyer Rd., Room 254
Monterey, CA 93943-5114

Dr. Russell L. Elsberry   80
Department of Meteorology, Code MR/Es
Naval Postgraduate School
589 Dyer Rd., Room 254
Monterey, CA 93943-5114

Library, Code 013   2
Naval Postgraduate School
Monterey, CA 93943-5100

Research Office, Code 09   1
Naval Postgraduate School
Monterey, CA 93943-5138

Defense Technical Information Center   2
8725 John J. Kingman Rd., STE 0944
Ft. Belvoir, VA 22060-6218